RESEARCH MEMORANDUM

THE EFFECT OF VARIOUS AERODYNAMIC BALANCES ON THE LOW-SPEED LATERAL-CONTROL AND HINGE-MOMENT CHARACTERISTICS OF A 0.20-CHORD PARTIAL-SPAN OUTBOARD AILERON ON A WING WITH LEADING EDGE SWEPT BACK 51.3°

By Alexander D. Hammond

Langley Aeronautical Laboratory
Langley Field, Va.

NATIONAL ADVISORY COMMITTEE
FOR AERONAUTICS

WASHINGTON

September 15, 1952

NACA RM L52G03

NATIONAL ADVISORY COMMITTEE FOR AERONAUTICS

RESEARCH MEMORANDUM

THE EFFECT OF VARIOUS AERODYNAMIC BALANCES ON THE LOW-SPEED LATERAL-CONTROL AND HINGE-MOMENT CHARACTERISTICS OF A 0.20-CHORD PARTIAL-SPAN OUTBOARD AILERON ON A WING WITH LEADING EDGE SWEPT BACK 51.3°

By Alexander D. Hammond

SUMMARY

A wind-tunnel investigation was made at low speeds to determine the lateral-control and hinge-moment characteristics of a 20-percent-chord, unsealed, partial-span outboard aileron equipped with either an overhang, a paddle, or a spoiler balance on a tapered 51.3° sweptback semispan wing model having an aspect ratio of 3.05.

The aileron effectiveness was relatively unaffected by the overhang or the paddle balance, but the spoiler balance generally increased the effectiveness obtained with the plain flap. A reduction in the hinge-moment coefficient was obtained with all the balances investigated, although the paddle and the spoiler balances gave a more favorable variation of hinge moment with aileron deflection and showed promise toward reduction of hinge moments to near-zero values.

INTRODUCTION

Excessive control hinge moments associated with the high speeds at which present-day aircraft operate have necessitated the extensive use of powered control systems. Although powered systems have proven to be adequate, a reduction in hinge moments is desirable either to cut down the size and weight of the boost system required or to provide controls that can be operated manually. The National Advisory Committee for Aeronautics is currently investigating several possible means of aerodynamically balancing excessive control hinge moments encountered in the transonic speed range. An exploratory investigation was initiated

at low speeds to study some of the characteristics of several types of aerodynamic balances on a wing having a plan form suitable for high-speed aircraft. Since very few hinge-moment data are available on lateral controls for wings of this plan form, the present investigation was made.

This paper presents the results of a preliminary investigation in the Langley 300 MPH 7- by 10-foot tunnel of the hinge moment and the effectiveness of an aileron equipped with either a plain radius nose, an overhang balance, a paddle balance, or a spoiler balance on an 8.5-percent-thick wing having a leading-edge sweepback of 51.3°, an aspect ratio of 3.05, and a taper ratio of 0.49. The 20-percent-chord by 39-percent-semispan aileron was flat-sided, unsealed, and extended from the 54-percent-semispan station outboard.

DEFINITIONS AND SYMBOLS

The forces and moments on the wing are presented about the wind axes, which, for the conditions of these tests (zero sideslip), correspond to the stability axes (fig. 1). The axes intersect the plane of symmetry at 27.8 percent mean aerodynamic chord as shown in figure 2.

The rolling-moment and yawing-moment coefficients determined on the semispan wing represent the aerodynamic effects that occur on a complete wing as the result of the deflection of one aileron. The lift, drag, and pitching-moment coefficients determined for the semispan wing (with the aileron neutral) represent those that occur for a complete wing.

The symbols used in the presentation of results are as follows:

C_L lift coefficient, $\frac{\text{Twice lift of semispan model}}{qS}$

C_D drag coefficient, $\frac{\text{Twice drag of semispan model}}{qS}$

C_m pitching-moment coefficient referred to $0.278\bar{c}$, $\frac{\text{Twice pitching moment of semispan model}}{qS\bar{c}}$

C_l rolling-moment coefficient, L/qSb

C_n yawing-moment coefficient, N/qSb

[redacted]

C_h aileron hinge-moment coefficient,

$$\frac{H_a}{2q \times \text{Area moment of aileron rearward of and about aileron hinge axis}}$$

b twice span of semispan model, 6.066 ft

S twice area of semispan model, 12.06 sq ft

A aspect ratio of wing, 3.05, b^2/S

L rolling moment due to aileron deflection, ft-lb

N yawing moment due to aileron deflection, ft-lb

H_a aileron hinge moment, ft-lb

q free-stream dynamic pressure, $\frac{1}{2}\rho V^2$, lb/sq ft

V free-stream velocity, ft/sec

ρ mass density of air, slug/cu ft

y lateral distance from plane of symmetry, ft

c local wing chord measured in planes parallel to wing plane of symmetry

c' local wing chord measured in planes perpendicular to wing 0.556c line

$\bar{c}$ wing mean aerodynamic chord (MAC), $\frac{2}{S}\int_0^{b/2} c^2 dy$, 2.087 ft

c_a local aileron chord measured along wing-chord plane from hinge axis of aileron to trailing edge of aileron in planes parallel to wing plane of symmetry

c_a' local aileron chord measured along wing-chord plane from hinge axis of aileron to trailing edge of aileron in planes perpendicular to 0.556c line

α angle of attack of chord plane at root of model, deg

[redacted]

δ_a aileron deflection, corrected for deflection under load, relative to wing-chord plane and measured in planes perpendicular to aileron hinge axis, deg

$$C_{h_\alpha} = \left(\frac{\partial c_h}{\partial \alpha}\right)_{\delta_a}$$

$$C_{h_{\delta_a}} = \left(\frac{\partial c_h}{\partial \delta_a}\right)_{\alpha}$$

$$C_{l_{\delta_a}} = \left(\frac{\partial c_l}{\partial \delta_a}\right)_{\alpha}$$

The subscripts δ_a and α outside the parentheses indicate the factor held constant. All slopes were measured in the vicinity of 0° angle of attack and 0° aileron deflection.

CORRECTIONS

All the test data have been corrected for jet-boundary and reflection-plane effects by the method of reference 1. Blockage corrections as determined from reference 2 to account for the constriction effects produced by the wing model and wing wake were also applied. Aileron deflections have been corrected for deflection under load, but the rolling-moment-coefficient data have not been corrected for the small amount of wing twist produced by the aileron deflection, since this correction as determined by static load tests was negligible. Reflection-plane corrections as determined from low-speed unpublished data have been applied to the rolling-moment data.

APPARATUS AND MODEL

The semispan sweptback wing was mounted vertically in the Langley 300 MPH 7- by 10-foot tunnel as shown in figure 3 with the ceiling serving as a reflection plane. The model was mounted on the balance system in such a manner that all forces and moments acting on the model could be measured. A small clearance gap was maintained between the model and the tunnel ceiling and a small end plate was attached to the root of the model to deflect the spanwise flow of air that enters the tunnel test section through the opening.

[redacted]

The model used for these tests was built of aluminum to the planform dimensions shown in figure 2. The model had an aspect ratio of 3.05, a taper ratio of 0.49, and a leading-edge sweepback of 51.3°. The wing sections perpendicular to the 55.6-percent-chord line had an NACA 65_1-012 airfoil profile. The aileron hinge moments were measured with an electric resistance-type strain gage.

The model was equipped with a 20-percent-chord by 39-percent semispan flat-sided, unsealed, plain-radius-nose aileron with the outboard end located 6.8 percent of the wing semispan inboard of the wing tip. The lateral-control and hinge-moment characteristics of the plain-radius-nose aileron and the aileron with several types of aerodynamic balances (fig. 4) were investigated. A description of these balances is given as follows:

(a) An elliptical and a sharp-nose overhang balance with 60-percent aileron chord overhang.

(b) An external delta-shaped paddle balance, located both above the upper and below the lower aileron surface.

(c) A spoiler balance projected along the 65-percent wing chord line extending from the inboard end of the aileron outboard. Spoiler spans of 37.5 and 50 percent of the aileron span were projected at the rate of 1 percent of the wing chord per 5° aileron deflection. Spoiler spans of 25-, 37.5-, and 50-percent span were projected at the rate of 2 percent per 5° δ_a.

TESTS

All the tests were made in the Langley 300 MPH 7- by 10-foot tunnel at an average dynamic pressure of 148.5 pounds per square foot, which corresponds to a Mach number of 0.328 and a Reynolds number of 4.45×10^6 based on the wing mean aerodynamic chord of 2.087 feet.

The lateral-control tests cover the deflection range from -30° to 30° and the angle-of-attack range from 0° to 28° for the various aerodynamic balances investigated.

[redacted]

RESULTS AND DISCUSSION

Wing Aerodynamic Characteristics

The aerodynamic characteristics in pitch of the wing, equipped with a flat-sided aileron, are presented in figure 5. Longitudinal aerodynamic characteristics through a range of Mach number from 0.302 to 0.913 are presented in reference 3 for the wing equipped with a true contour (cusped trailing edge) aileron. The aerodynamic characteristics (fig. 5) are in good agreement with the aerodynamic characteristics at low Mach numbers presented and discussed in reference 3. For this reason the aerodynamic characteristics in pitch are not discussed in the present paper.

Curves of the variation of drag coefficient with lift coefficient for the plain-radius-nose aileron and the aileron with the various balances are presented in figure 6. The scale for this figure has been expanded in order to show the increment in drag caused by the addition of the balances. It can be seen from this figure that the additional drag caused by any of the balances investigated when the aileron is in the neutral or trim position is small.

Lateral-Control and Hinge-Moment Characteristics

The variation of the lateral-control and hinge-moment characteristics with aileron deflection at various angles of attack for the plain-radius-nose aileron and the aileron with the various aerodynamic balances is presented in figures 7 to 9 and summarized in figure 10. The lateral-control and hinge-moment parameters $C_{l_{\delta_a}}$, C_{h_α}, and $C_{h_{\delta_a}}$ determined from the data in figures 7 to 10 are presented in table I.

Rolling-moment characteristics.- Except for angles of attack near stall and large aileron deflections, the rolling-moment coefficients of the aileron equipped with the various balances investigated varied almost linearly with aileron deflection (figs. 7 to 10). The aileron effectiveness parameters were relatively unaffected by the size or shape of the overhang balance or by the addition of the paddle balance (table I). Projection of the spoiler in front of the aileron at the rate of 2 percent of the wing chord per 5° aileron deflection, however, increased the aileron effectiveness parameter $C_{l_{\delta_a}}$. In general, the increase in rolling effectiveness resulting from the projection of a spoiler in front of the aileron became larger as the span of the spoiler was increased.

[redacted]

Hinge-moment characteristics.- The aileron equipped with any of the various aerodynamic balances investigated showed a fairly linear variation of hinge-moment coefficient C_h with angle of attack at 0° aileron deflection below approximately 8° angle of attack (fig. 10). It can be further seen from figures 7 to 9 that this linear variation holds true through the ±10° aileron-deflection range at these angles of attack. Except for the aileron with the $0.60c_a$ overhang balances or the paddle balances, the values of C_h at a given aileron deflection generally became more negative as the angle of attack was increased to approximately 21°. The hinge-moment parameter C_{h_α} (measured near zero angle of attack) for the aileron with the paddle balance or the $0.60c_a$ overhang balances generally was slightly positive throughout most of the deflection range investigated (figs. 7 to 10). It should be remembered that positive values of C_{h_α} tend to increase the stick force during maneuvers and should, therefore, be considered when evaluating the different aerodynamic balances.

The aileron with the various aerodynamic balances also showed a fairly linear variation of C_h with aileron deflection in the ±10° deflection range for angles of attack below 16.6°. Except for the aileron with the $0.60c_a$ overhang balances or the spoiler balances projected at the rate of 0.02c per 5° δ_a, the values of C_h at a given angle of attack, below approximately 21° (figs. 7 to 10), generally increased negatively as the aileron deflection was increased positively (denoting an underbalanced control) throughout the deflection range. The aileron with the $0.60c_a$ elliptical nose overhang became overbalanced above approximately ±10° δ_a and the aileron with the $0.60c_a$ sharp-nose overhang becomes overbalanced above approximately -20° δ_a (figs. 7(b), 7(c), and 10(a)). It should be noted that the aileron deflections at which the aileron with the $0.60c_a$ overhang balances became overbalanced correspond very nearly to the deflections at which the elliptical or the sharp nose emerged from the wing contour. The aileron with the spoiler balance projected at the rate of 2 percent per 5° δ_a became overbalanced above approximately ±10° δ_a for the $\frac{3}{8}$-aileron-span spoiler balance and was overbalanced throughout the aileron-deflection range for the one-half aileron span spoiler balance (figs. 9(d), 9(e), and 10(c)).

An increase in the span or rate of projection of the spoiler balances increases the balancing power of the spoiler balances (fig. 10(c)). The reductions in the hinge-moment coefficients of the aileron with the various spoiler balances measured in this investigation result from the change in loading over the aileron with spoiler projection. Further reduction in the aileron hinge-moment coefficients resulting in the use

[redacted]

of smaller spoiler spans or in smaller rates of spoiler projection could be obtained by linking the spoiler to the aileron so that the hinge moments of the ailerons are balanced by those of the spoiler. The results of such an investigation are presented in reference 4.

All the aerodynamic balances gave appreciable reductions in the hinge-moment coefficients of the plain-radius-nose aileron at low speeds. The spoiler balances, however, have the most favorable variation of hinge moment with aileron deflection and indicate that at a given speed the hinge moment of the aileron can be reduced to near zero without overbalance for the large aileron deflections.

It should be stressed that the balance configurations investigated were not necessarily the optimum but that the data thus obtained in conjunction with section data (ref. 5, for example) can be used to estimate the amount of balance needed to obtain near-zero hinge moments.

CONCLUSIONS

A wind-tunnel investigation made at low speeds to determine the lateral-control and hinge-moment characteristics of a partial-span aileron having various aerodynamic balances on a 51.3° sweptback semispan wing indicated the following:

1. The aileron effectiveness was relatively unaffected by the size or shape of the overhang balance or by the addition of the paddle balance, but projection of a spoiler in front of the aileron as an aerodynamic balance generally resulted in an increase in the aileron effectiveness.

2. All the aerodynamic balances gave appreciable reductions in the hinge-moment coefficients of the plain-radius-nose aileron at low speeds. The spoiler balance and the paddle balance, however, have the most favorable variations of hinge moment with aileron deflection and indicate that at a given speed the hinge moment of the aileron can be reduced to near zero without overbalance occurring for the large aileron deflections. These balances are recommended for further investigation.

Langley Aeronautical Laboratory
National Advisory Committee for Aeronautics
Langley Field, Va.

[redacted]

REFERENCES

1. Polhamus, Edward C.: Jet-Boundary-Induced-Upwash Velocities for Swept Reflection-Plane Models Mounted Vertically in 7- by 10-Foot, Closed, Rectangular Wind Tunnels. NACA TN 1752, 1948.

2. Herriot, John G.: Blockage Corrections for Three-Dimensional-Flow Closed-Throat Wind Tunnels, With Consideration of the Effect of Compressibility. NACA Rep. 995, 1950. (Supersedes NACA RM A7B28.)

3. Schneiter, Leslie E., and Hagerman, John R.: Wind-Tunnel Investigation at High Subsonic Speeds of the Lateral-Control Characteristics of an Aileron and a Stepped Spoiler on a Wing With Leading Edge Swept Back 51.3°. NACA RM L9D06, 1949.

4. Lockwood, Vernard E., and Fikes, Joseph E.: Control Characteristics at Transonic Speeds of a Linked Flap and Spoiler on a Tapered 45° Sweptback Wing of Aspect Ratio 3. NACA RM L52D25, 1952.

5. Sears, Richard I.: Wind-Tunnel Data on the Aerodynamic Characteristics of Airplane Control Surfaces. NACA ACR 3L08, 1943.

[redacted]

TABLE I

SUMMARY OF THE LATERAL-CONTROL CHARACTERISTICS

OF A 20-PERCENT-CHORD AILERON WITH

VARIOUS AILERON BALANCES

Configuration	$C_{h_{\delta_a}}$	C_{h_α}	$C_{l_{\delta_a}}$
Plain radius-nose overhang	-0.0031	-0.0002	-0.00050
$0.60c_a$ elliptical-nose overhang	-.0013	.0011	-.00047
$0.60c_a$ sharp-nose overhang	-.0013	.0009	-.00050
Paddle balance on both aileron surfaces	-.0011	.0013	-.00055
3/8 aileron span spoiler projected 0.01c per 5° δ_a	-.0023	-.0002	-.00050
1/2 aileron span spoiler projected 0.01c per 5° δ_a	-.0018	-.0002	-.00056
1/4 aileron span spoiler projected 0.02c per 5° δ_a	-.0011	-.0002	-.00060
3/8 aileron span spoiler projected 0.02c per 5° δ_a	-.0008	-.0002	-.00068
1/2 aileron span spoiler projected 0.02c per 5° δ_a	+.0025	-.0002	-.00072

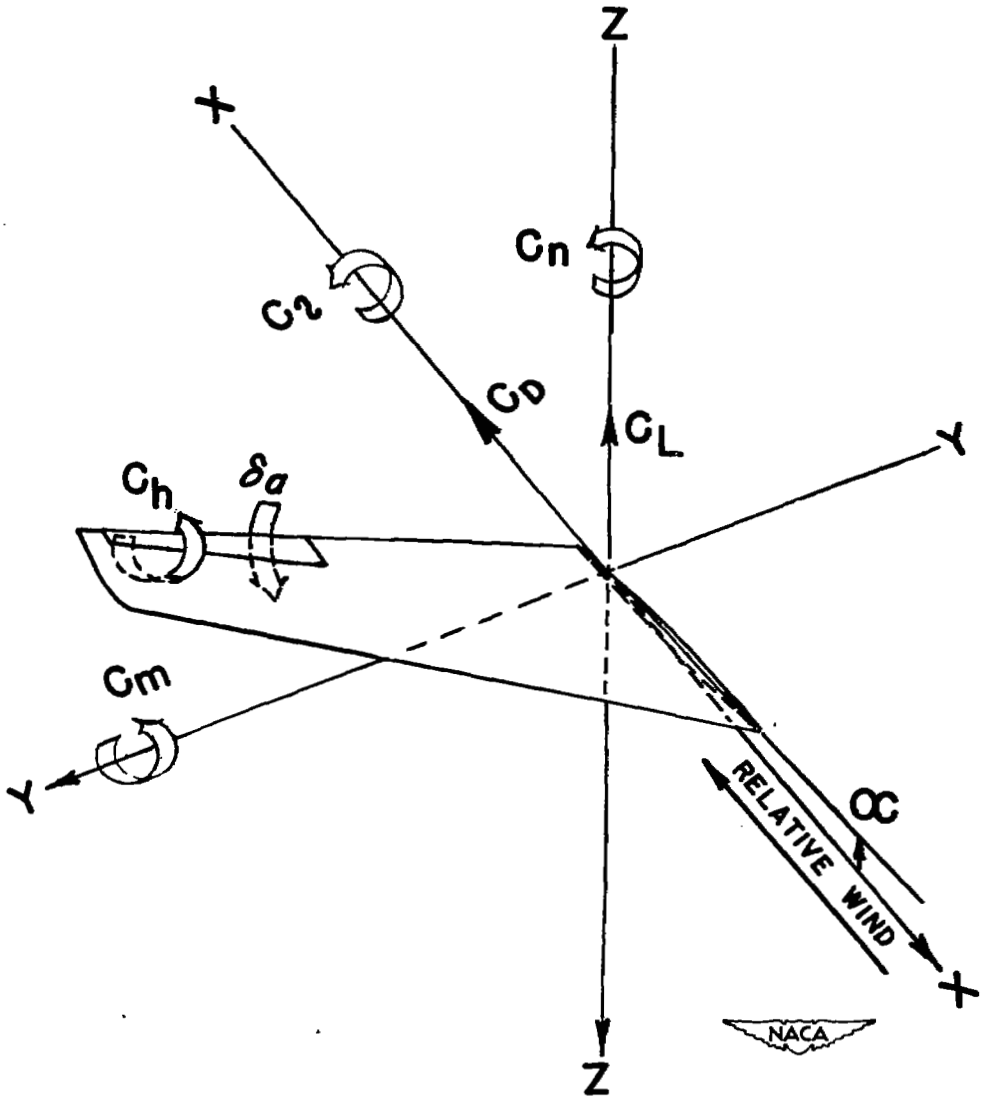

Figure 1.- System of axes, control surface hinge moments, and deflections. Positive direction of forces, moments, and deflection are indicated by the arrows.

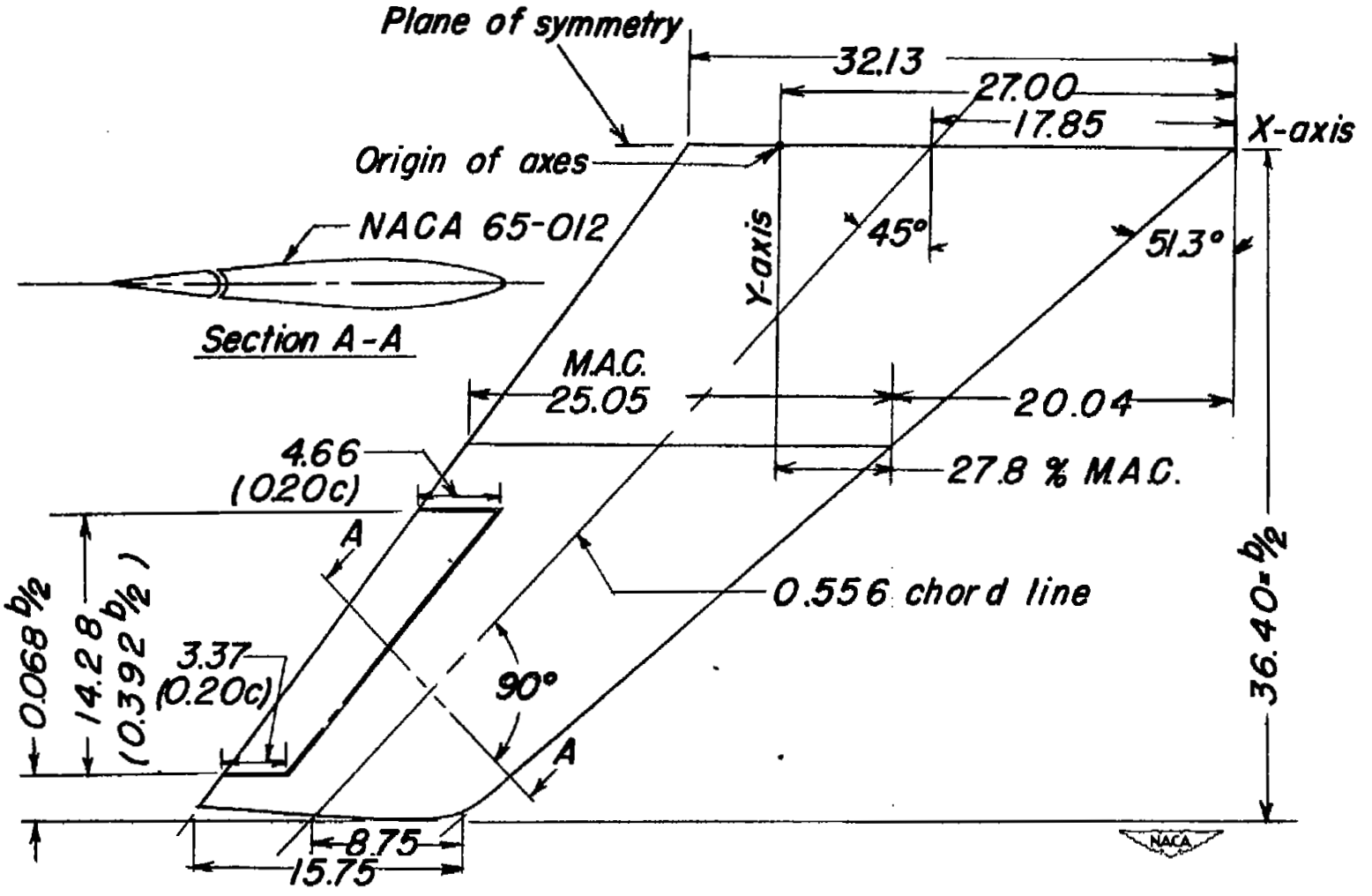

Figure 2.- Arrangement of the aileron on the 51.3° sweptback semispan wing. A = 3.06; S = 12.06 square feet; taper ratio 0.49. (All dimensions are in inches unless otherwise noted.)

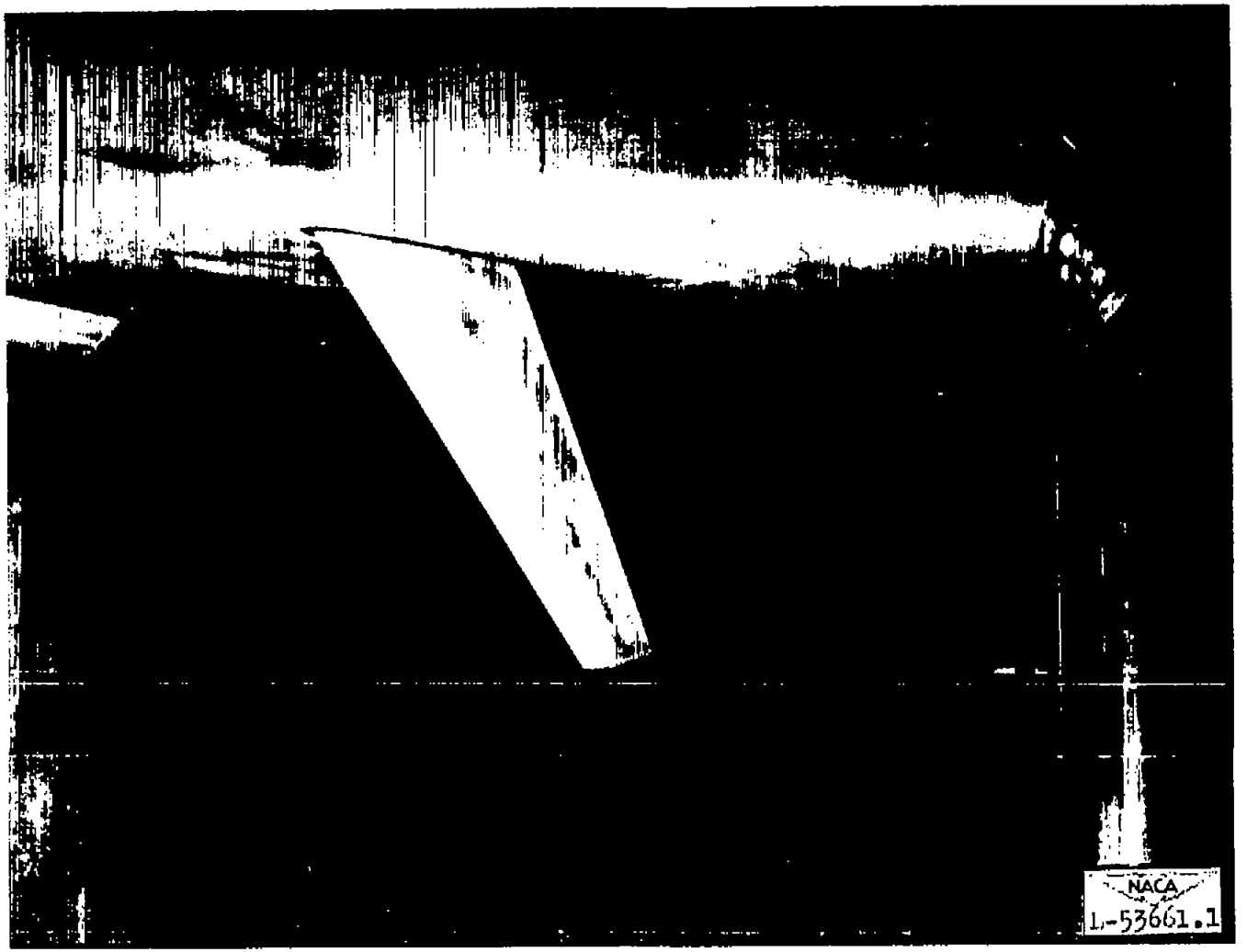

Figure 3.- The 51.3° sweptback semispan wing mounted vertically in the Langley 300 MPH 7- by 10-foot tunnel.

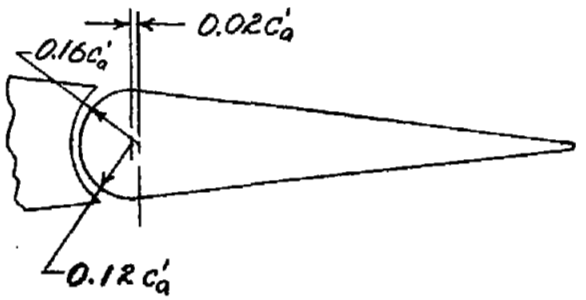

(a) Plain-radius-nose aileron.

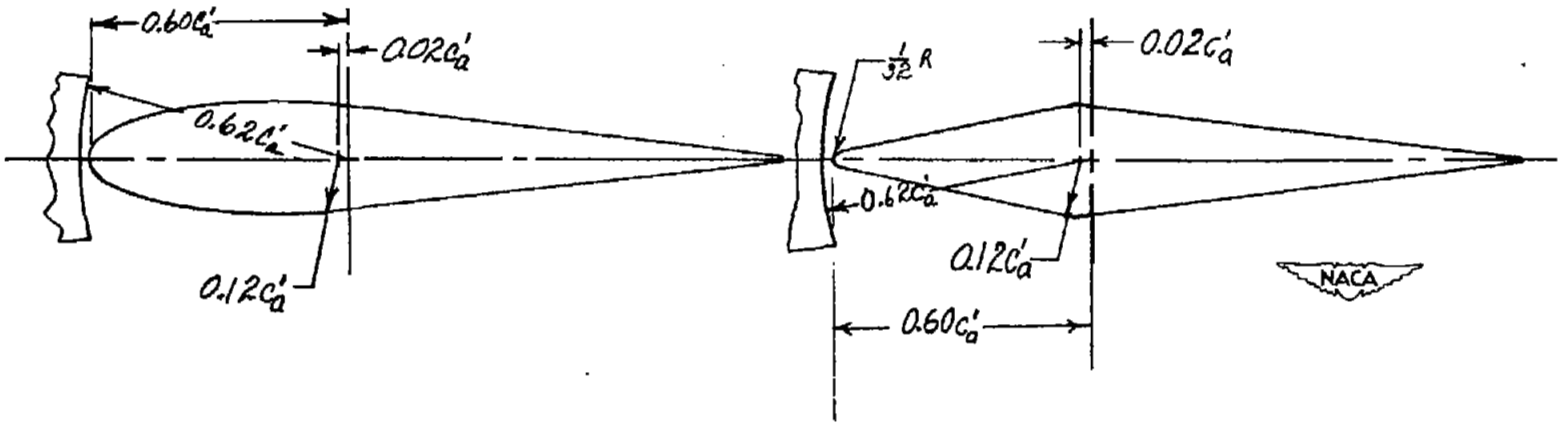

(b) Plain-radius-nose aileron and overhang balance.

Figure 4.- The plain-radius-nose aileron and the various aerodynamic balances investigated on the 20-percent-chord by 39-percent-semispan aileron.

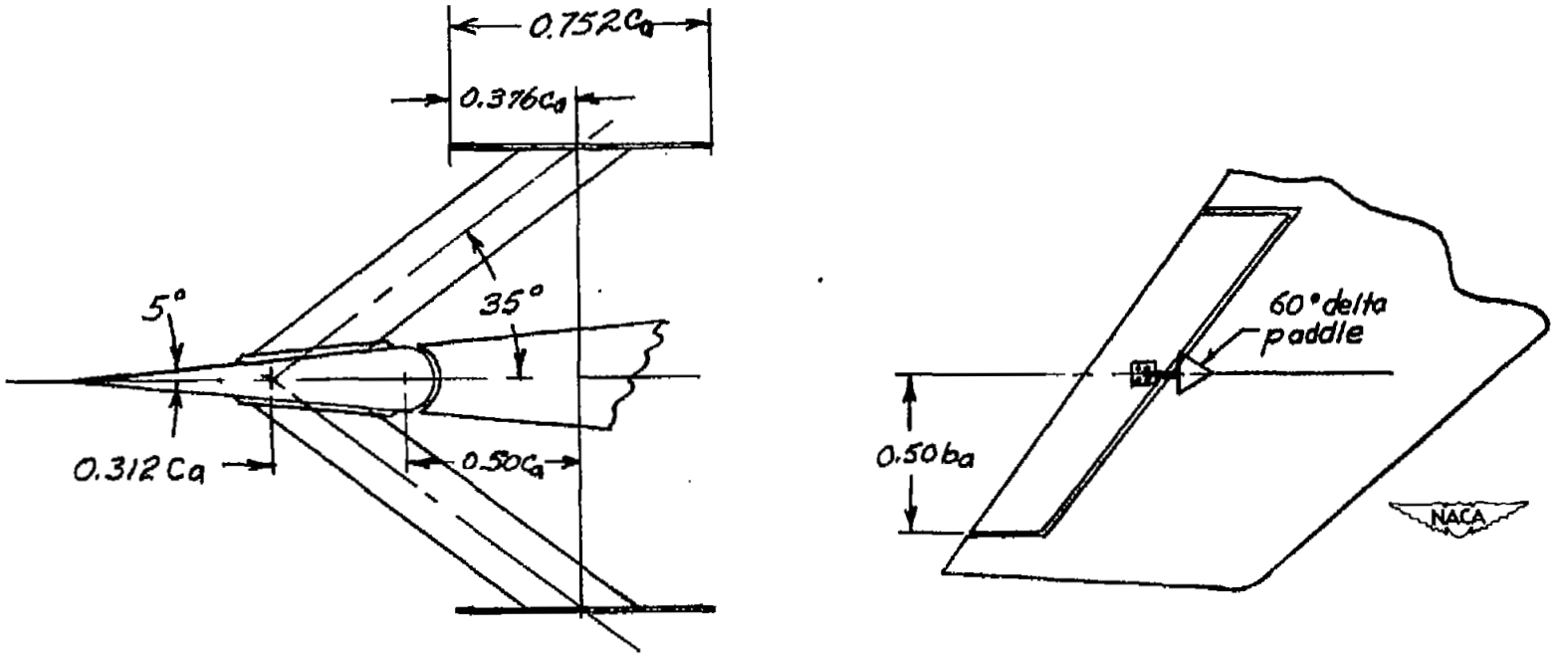

(c) Paddle balance.

Figure 4.- Continued.

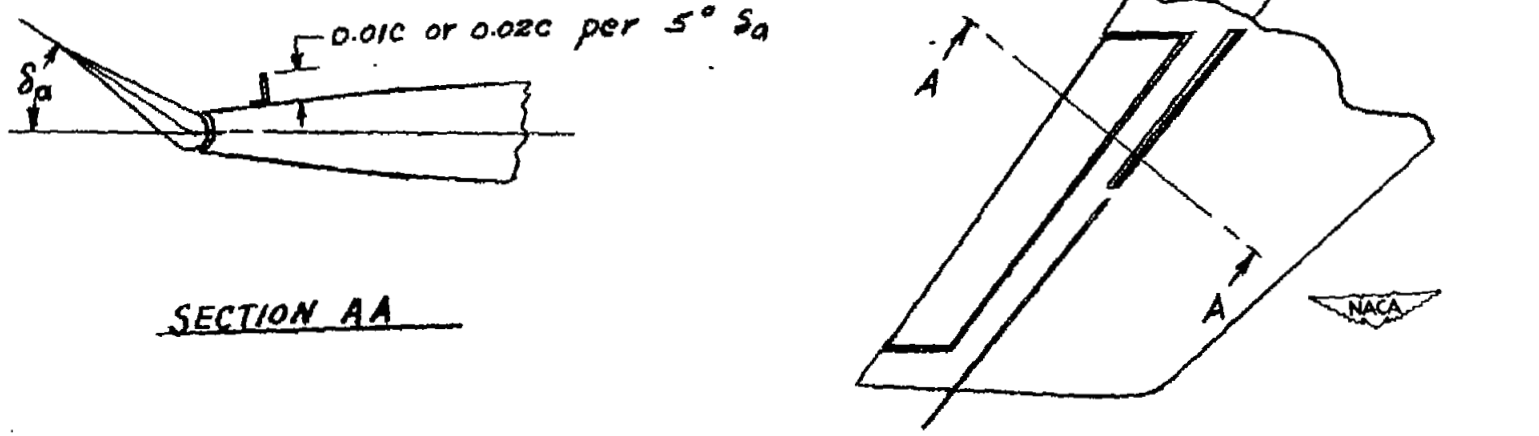

(d) Spoiler balance.

Figure 4.- Concluded.

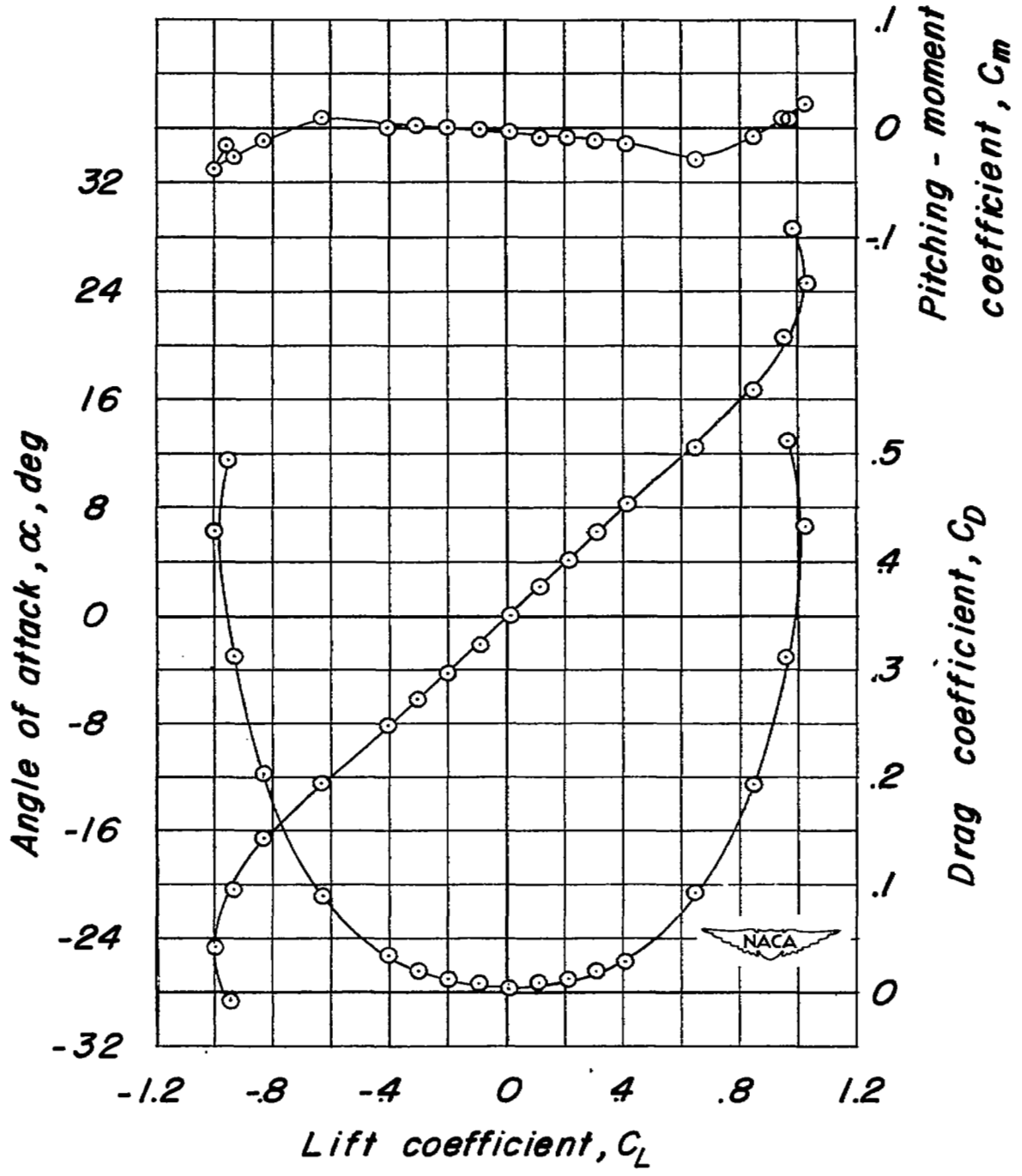

Figure 5.- The aerodynamic characteristics in pitch of 51.3° sweptback wing with $\delta_a \approx 0°$.

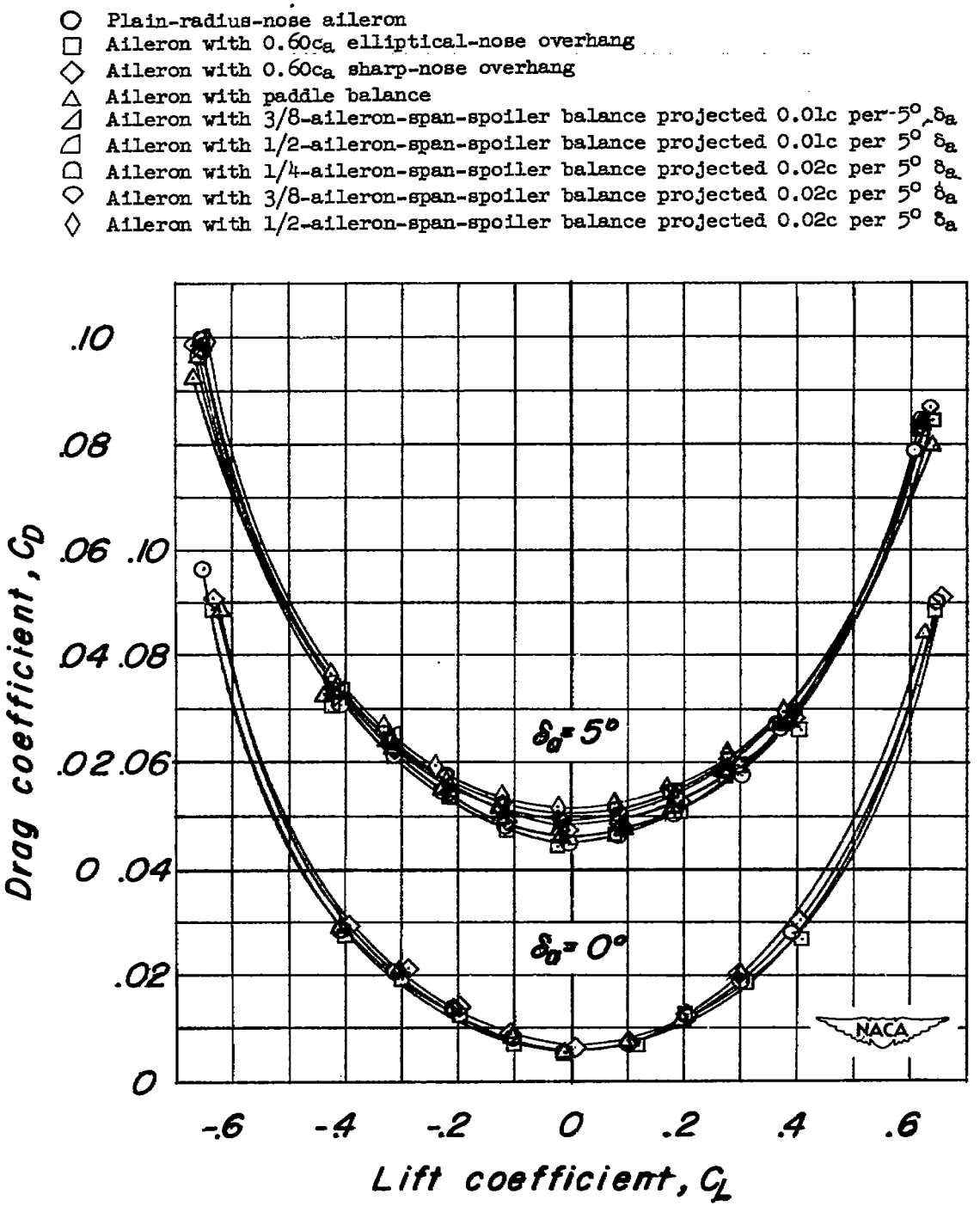

Figure 6.- The variation of drag coefficient with lift coefficient for the plain-radius-nose aileron and the aileron with various aerodynamic balances.

[redacted]

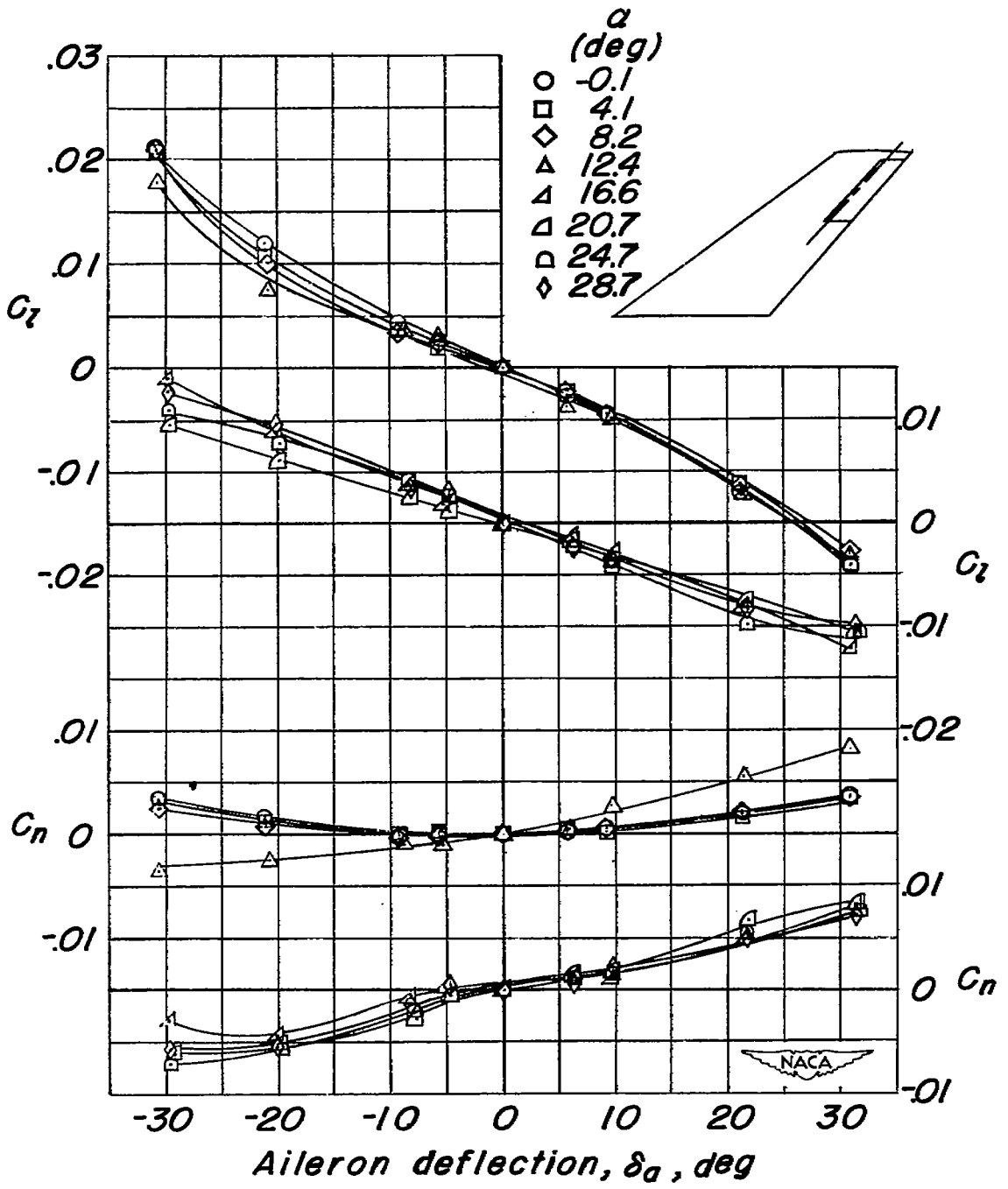

(a) Plain-radius-nose aileron.

Figure 7.- Variation of the lateral control and hinge moment characteristics with aileron deflection for the plain-radius-nose aileron and the aileron equipped with various overhang balances. M = 0.33.

[redacted]

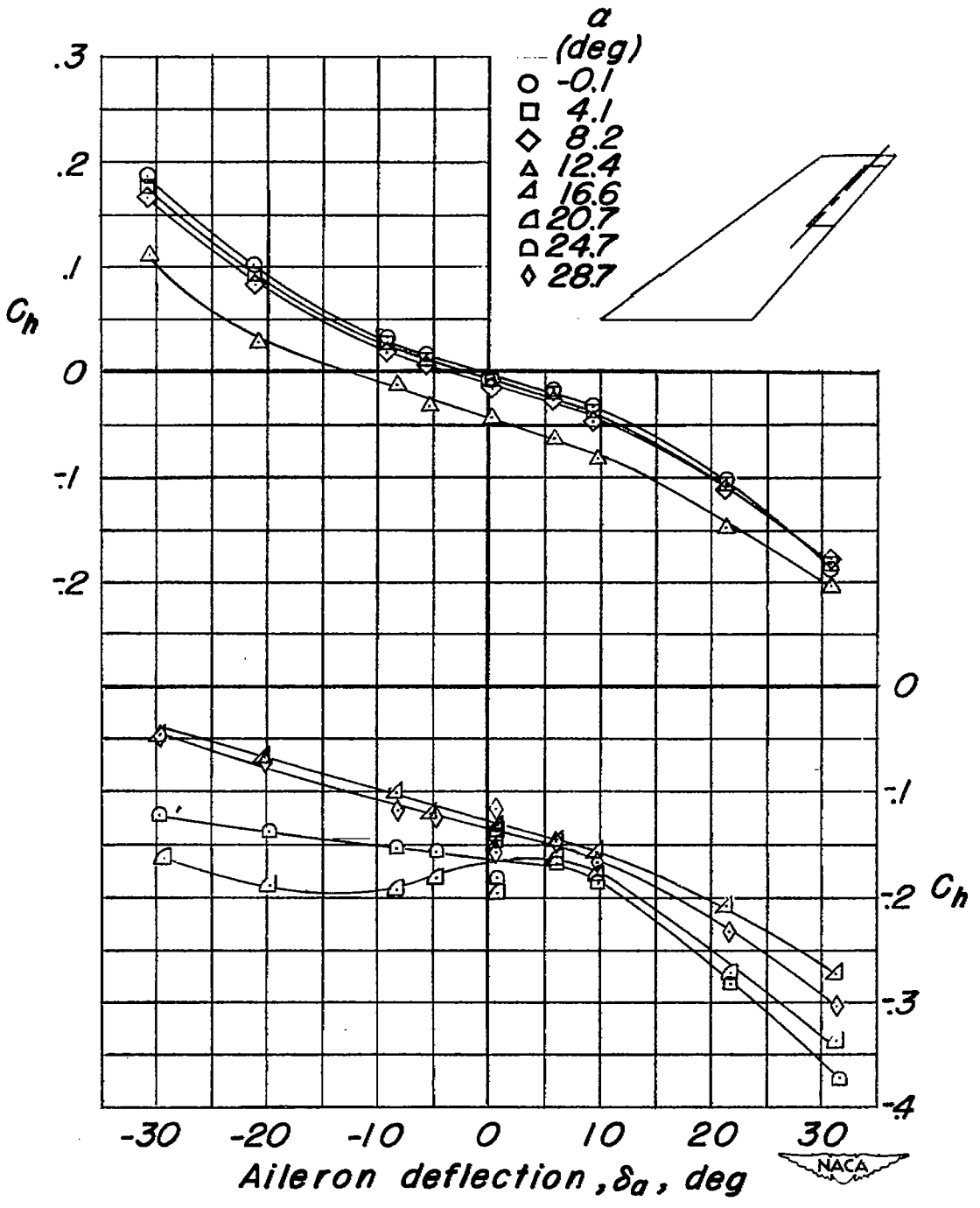

(a) Concluded.

Figure 7.- Continued.

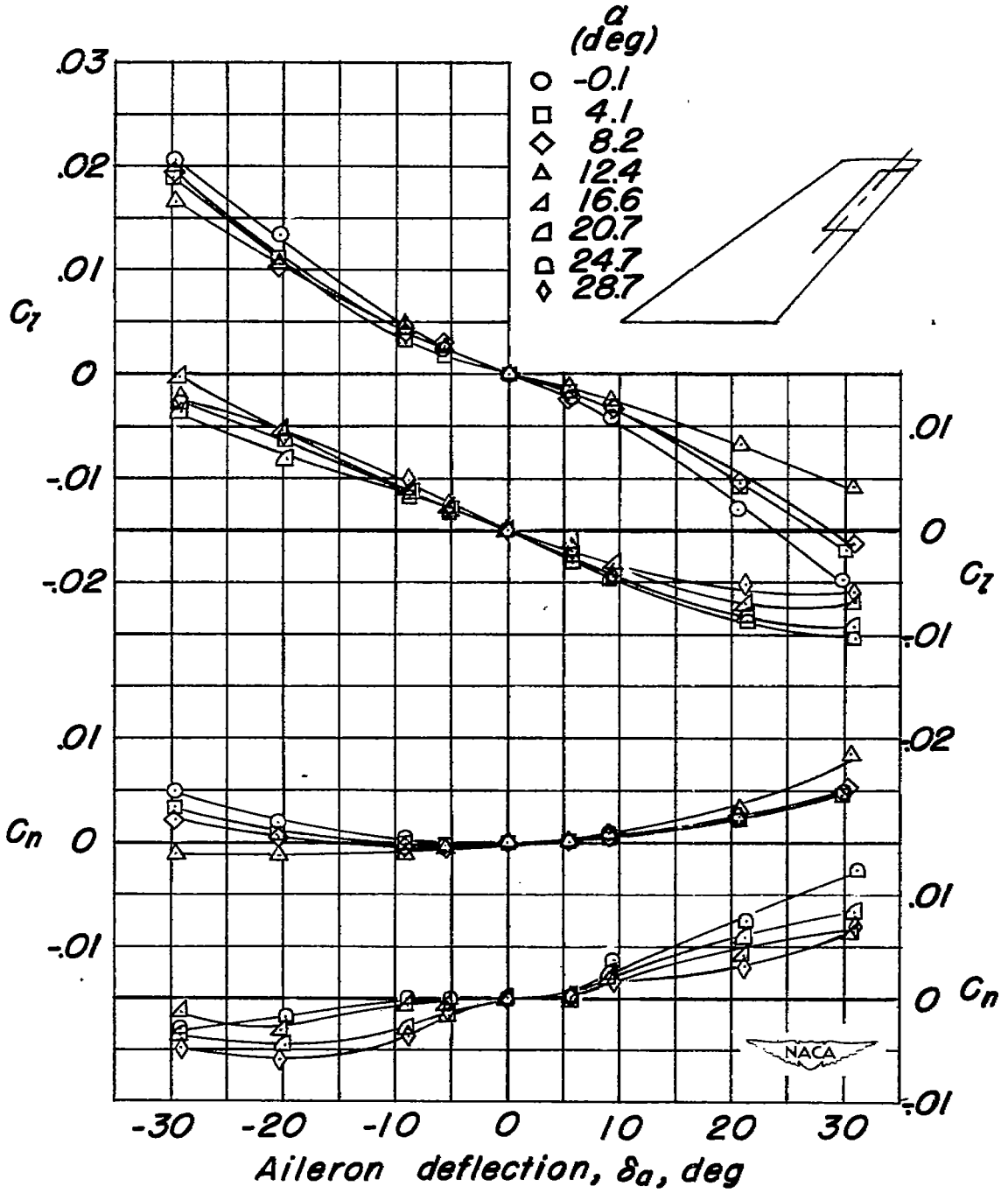

(b) An $0.60c_a$ elliptical-nose overhang.

Figure 7.- Continued.

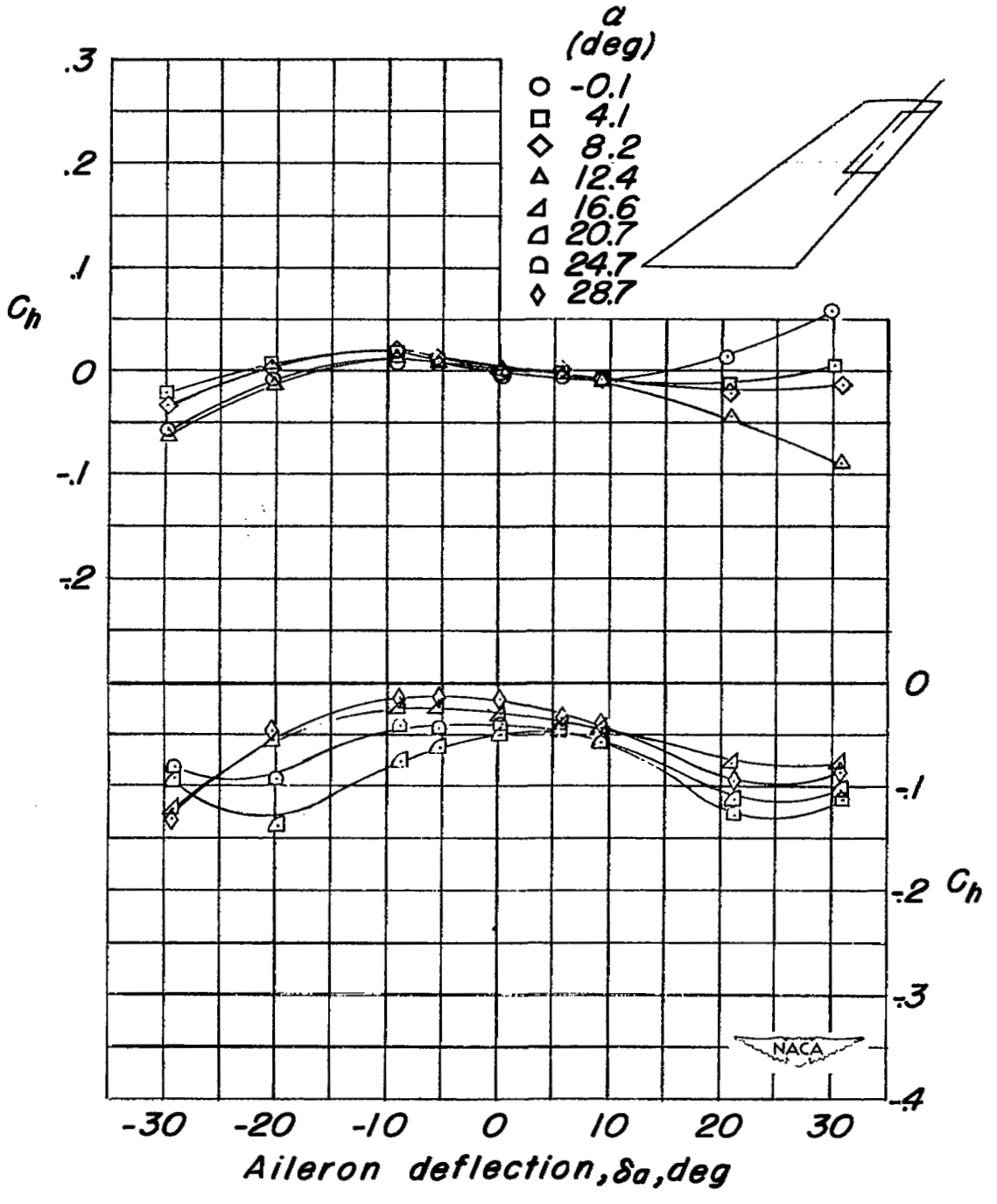

(b) Concluded.

Figure 7.- Continued.

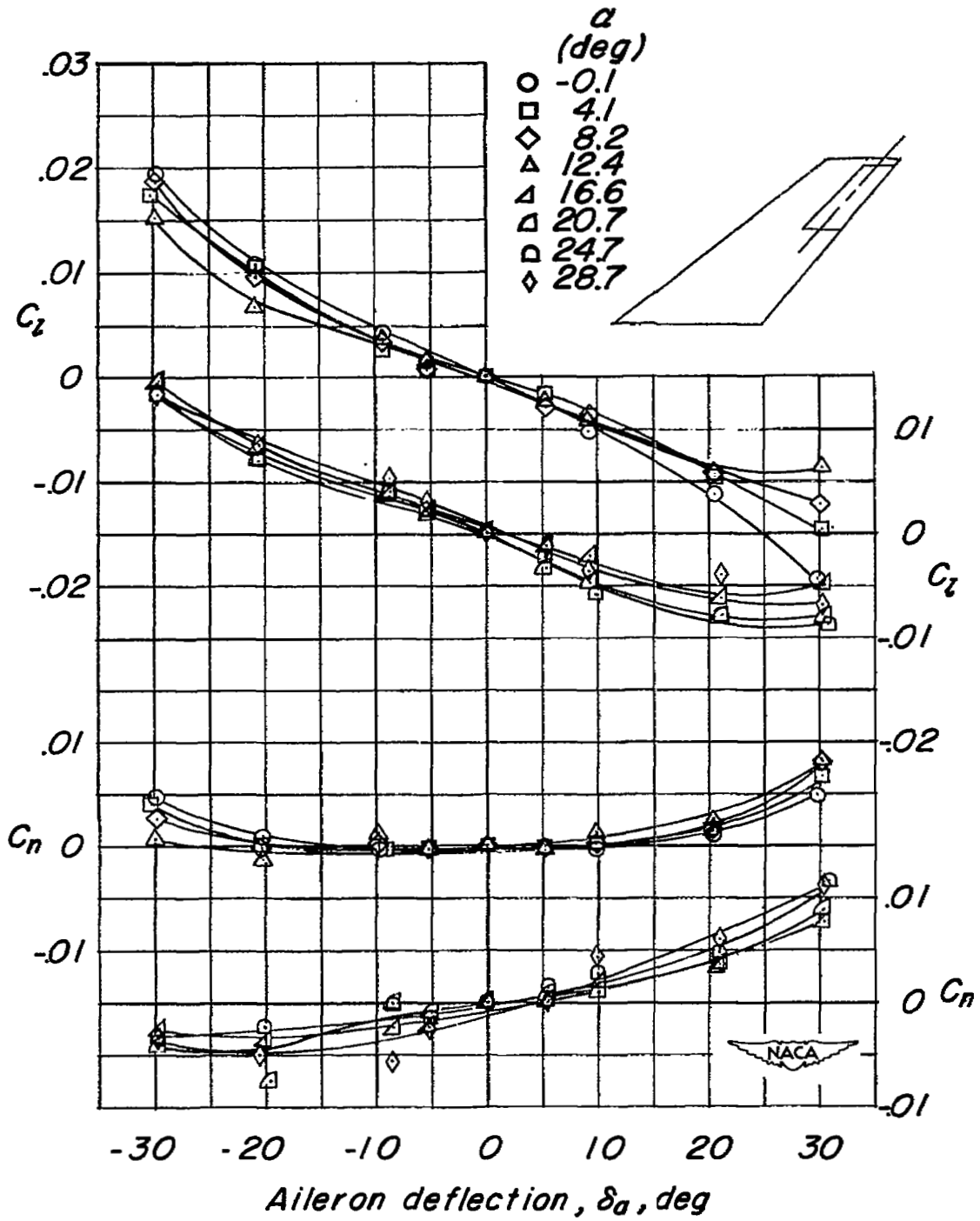

(c) An $0.60c_a$ sharp-nose overhang.

Figure 7.- Continued.

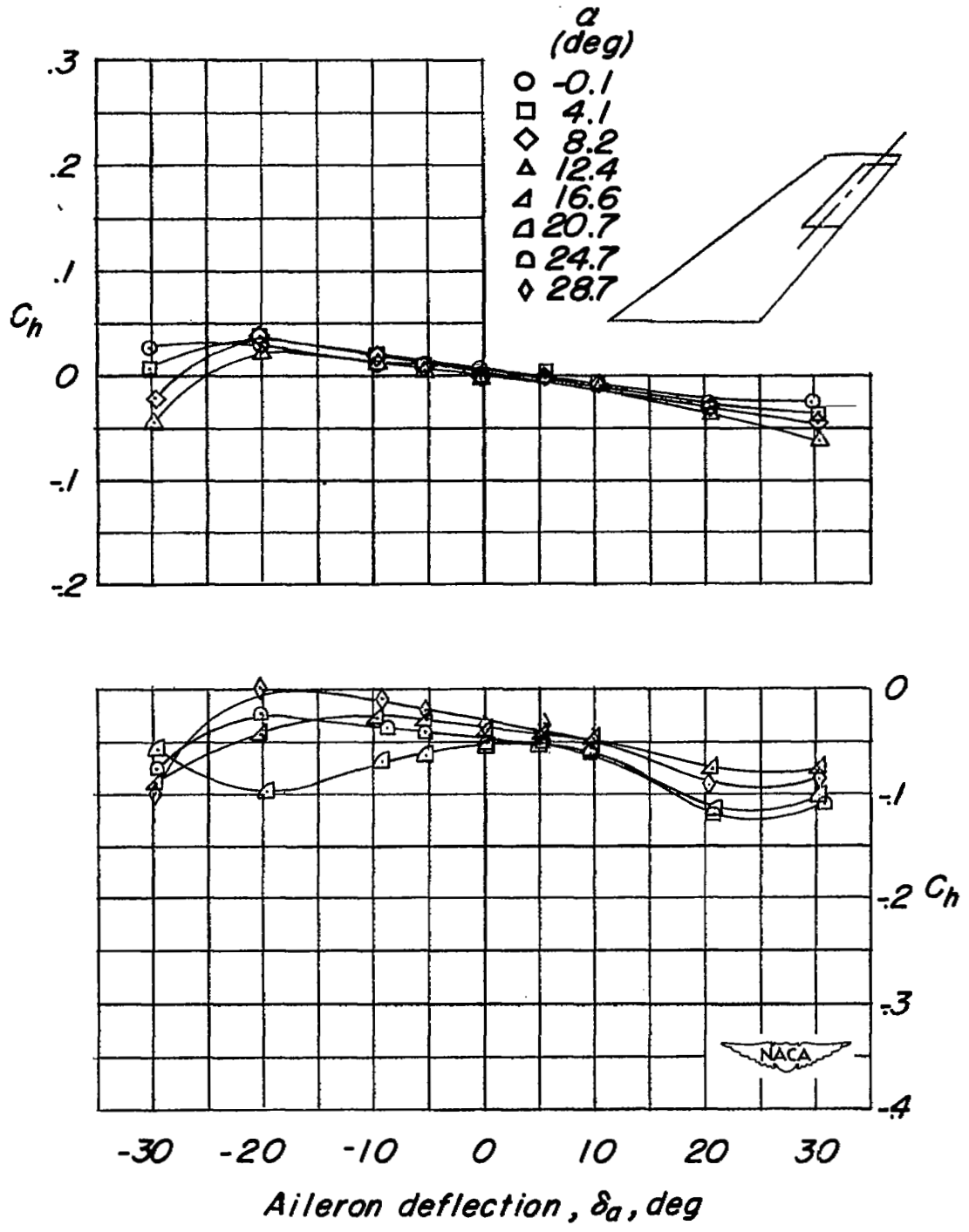

(c) Concluded.

Figure 7.- Concluded.

[redacted]

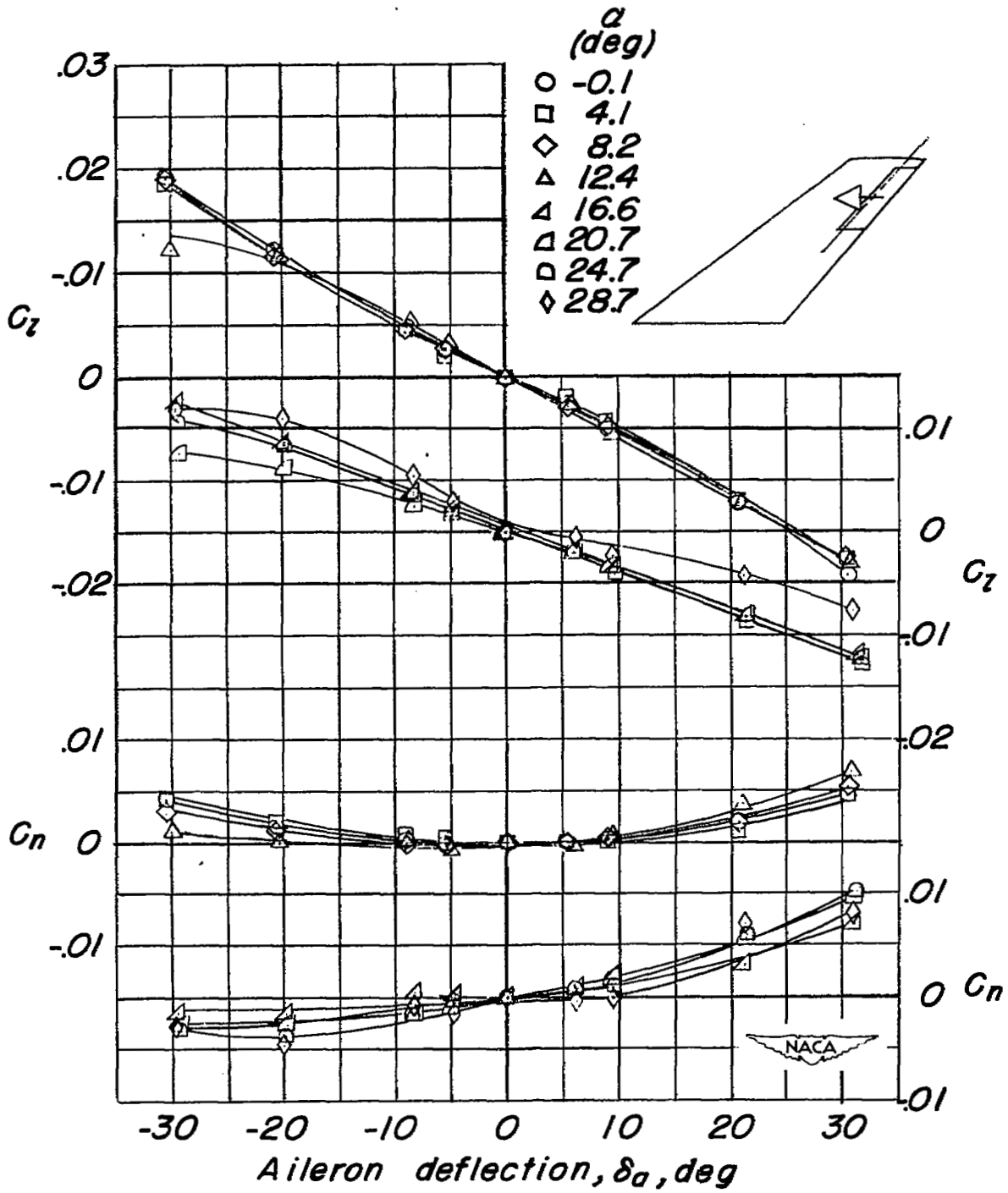

Figure 8.- Variation of the lateral-control and hinge-moment characteristics with aileron deflection for the plain-radius-nose aileron equipped with a paddle balance.

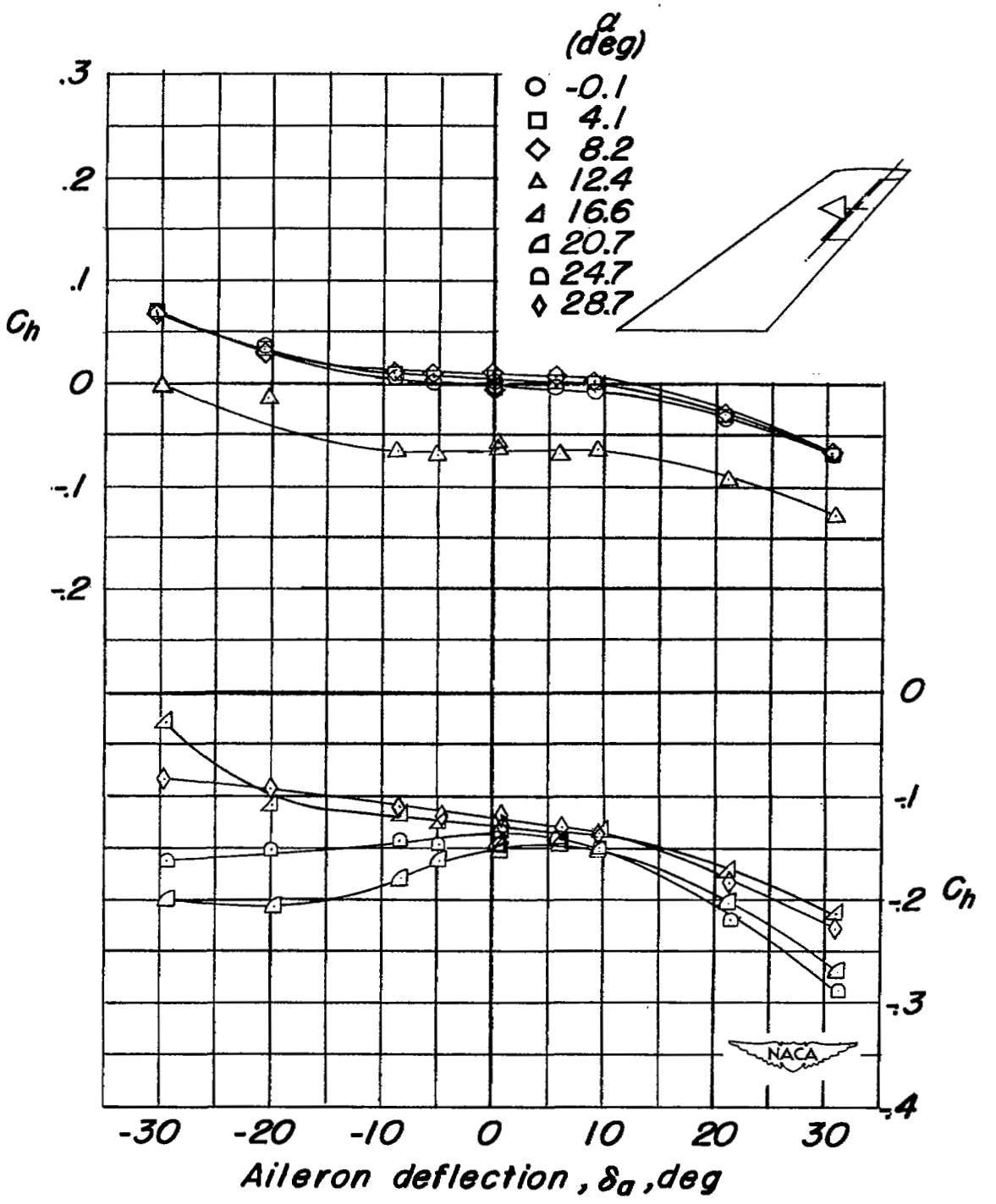

Figure 8.- Concluded.

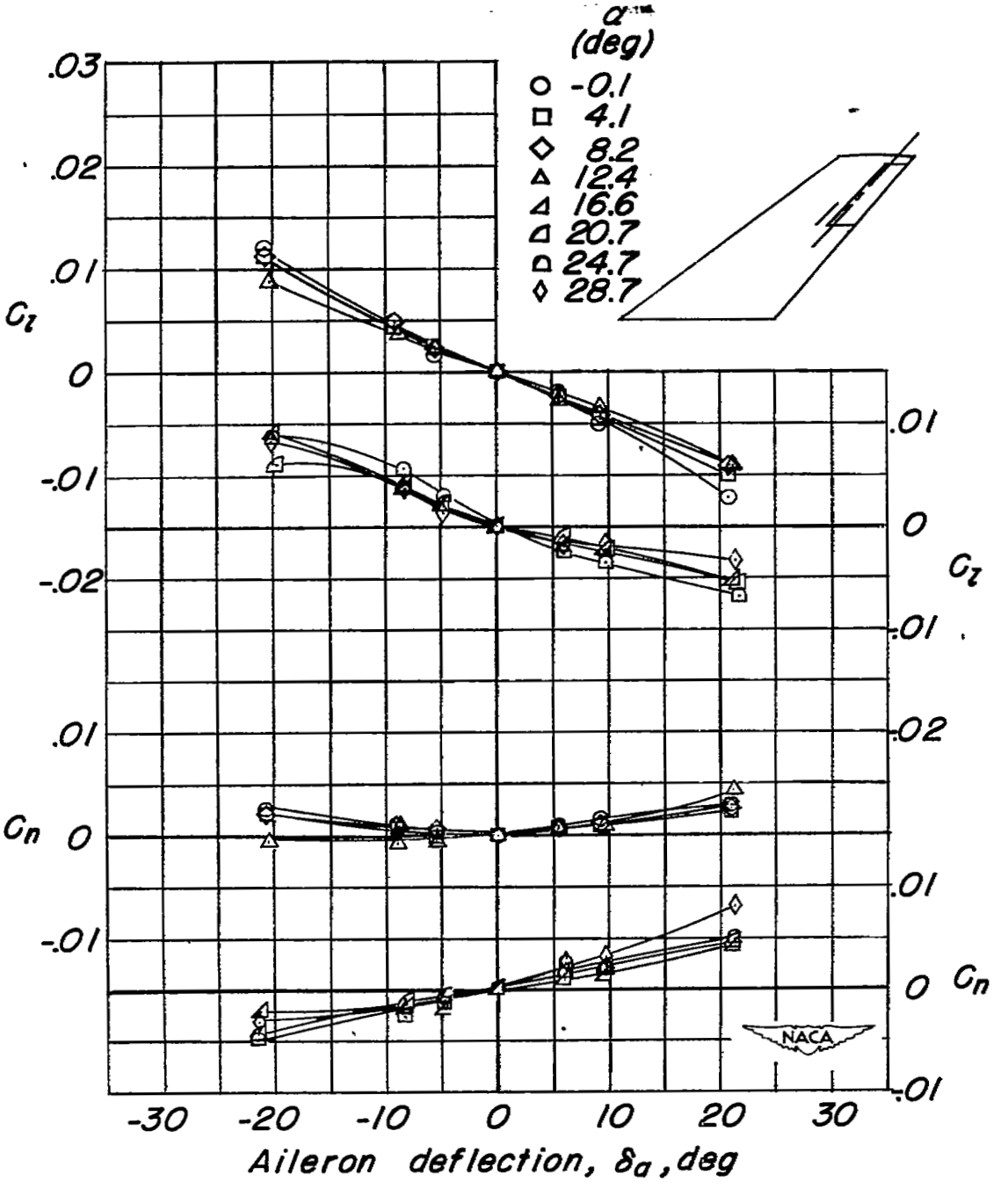

(a) Three-eights-aileron-span spoiler projected 0.01c per 5° δ_a.

Figure 9.- Variation of the lateral-control and hinge-moment characteristics with aileron deflection for the plain-radius-nose aileron with various spoiler-type balances.

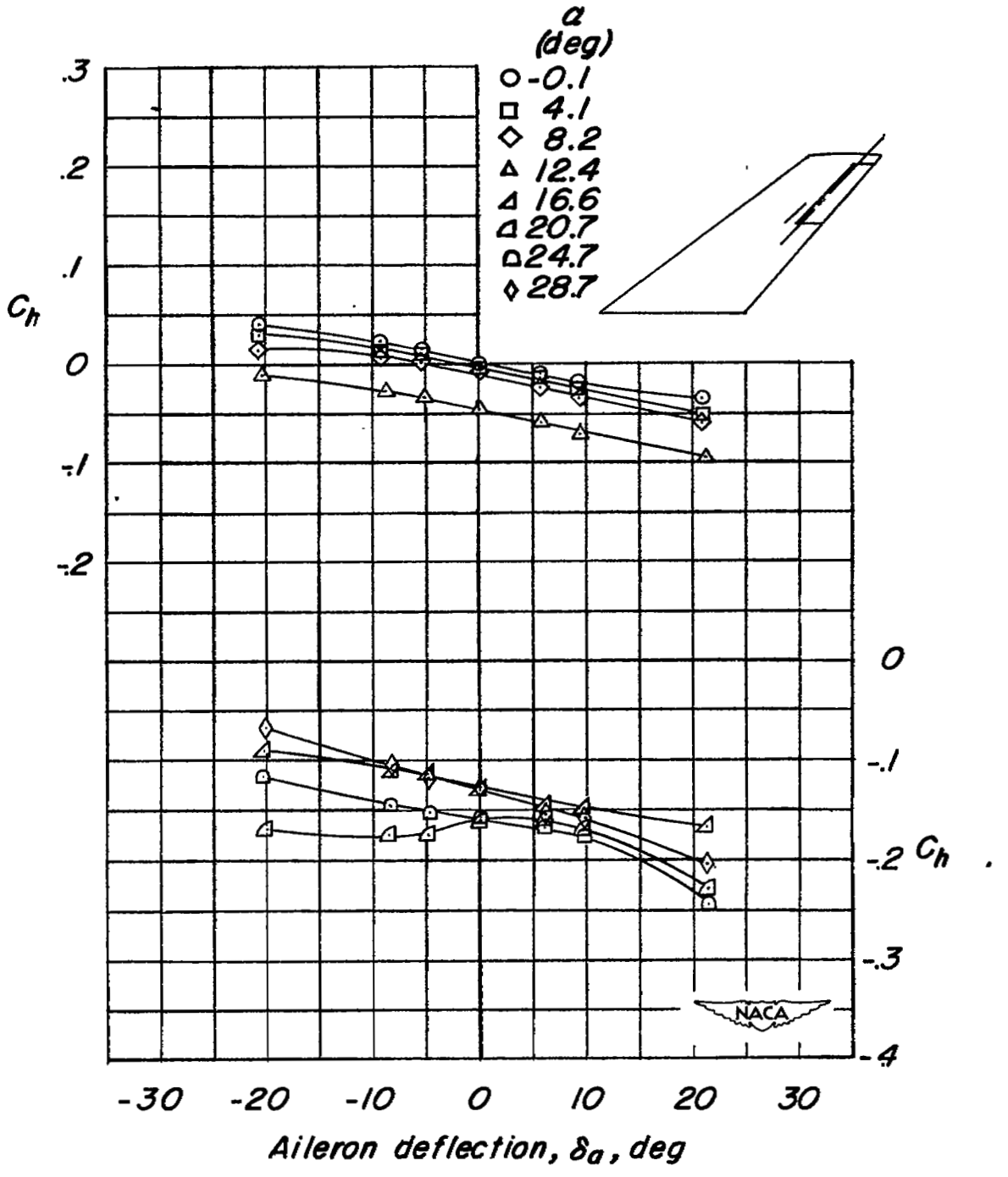

(a) Concluded.

Figure 9.- Continued.

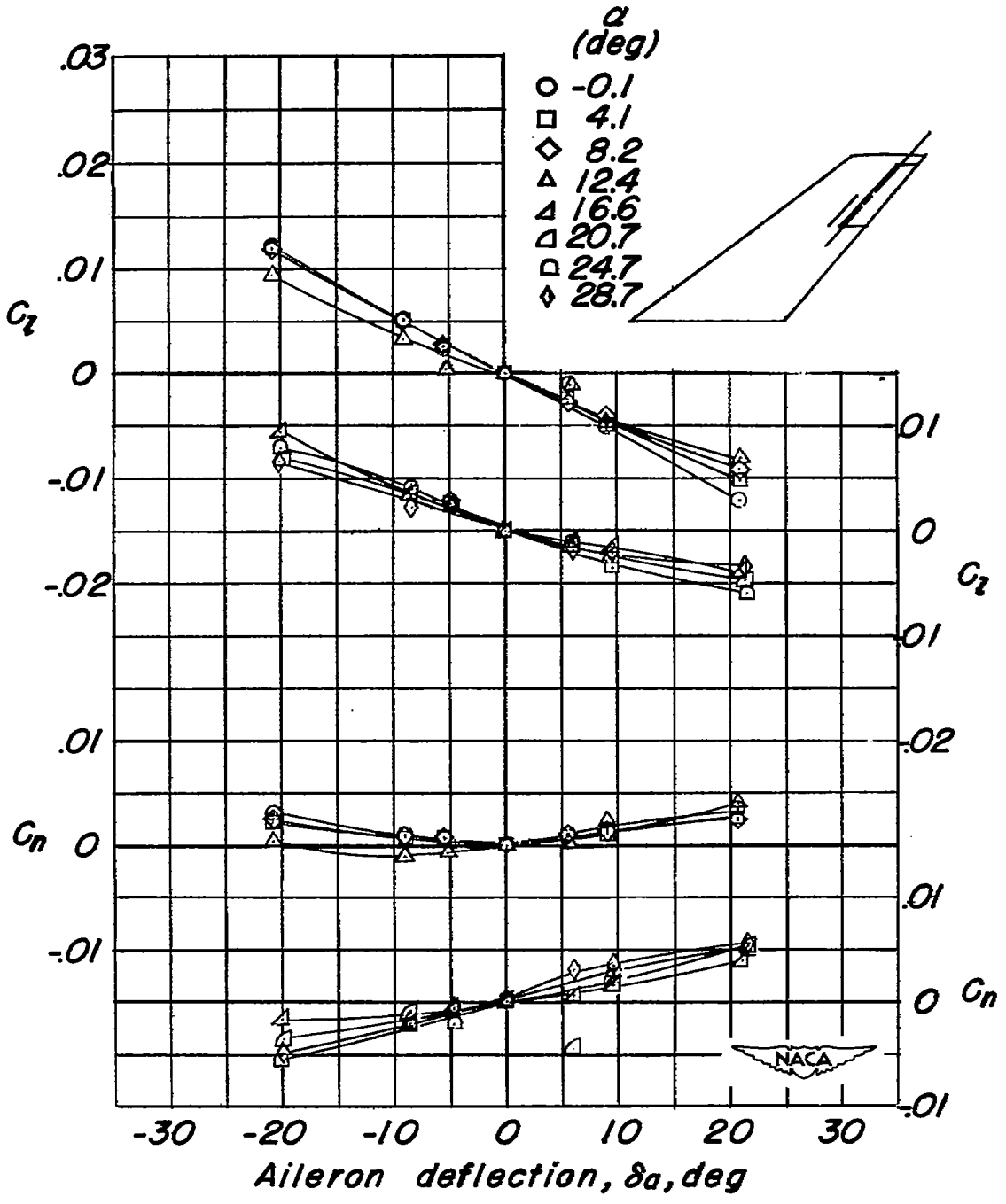

(b) One-half-aileron-span spoiler projected 0.01c per 5° δ_a.

Figure 9.- Continued.

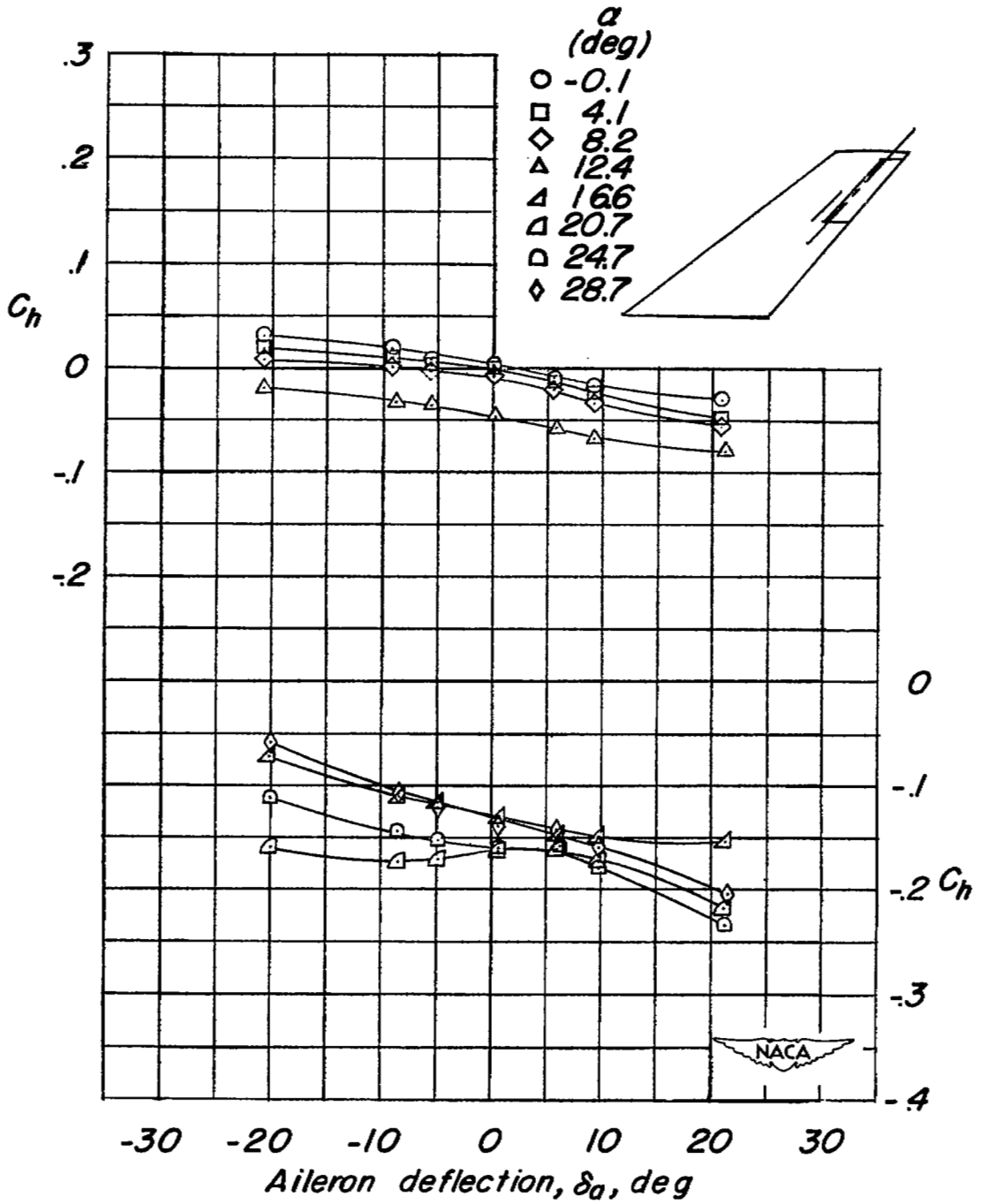

(b) Concluded.

Figure 9.- Continued.

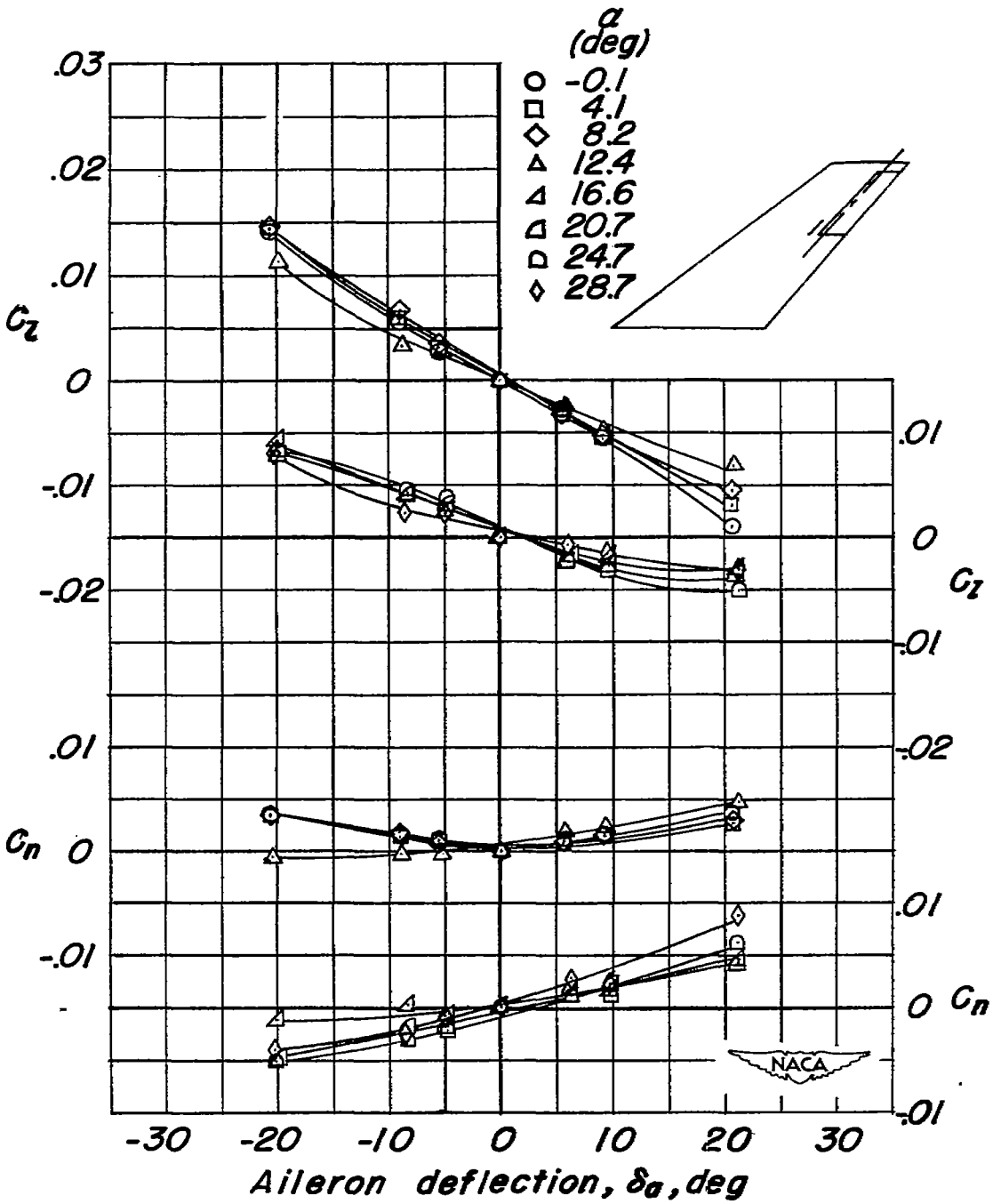

(c) One-fourth-aileron-span spoiler projected 0.02c per 5° δ_a.

Figure 9.- Continued.

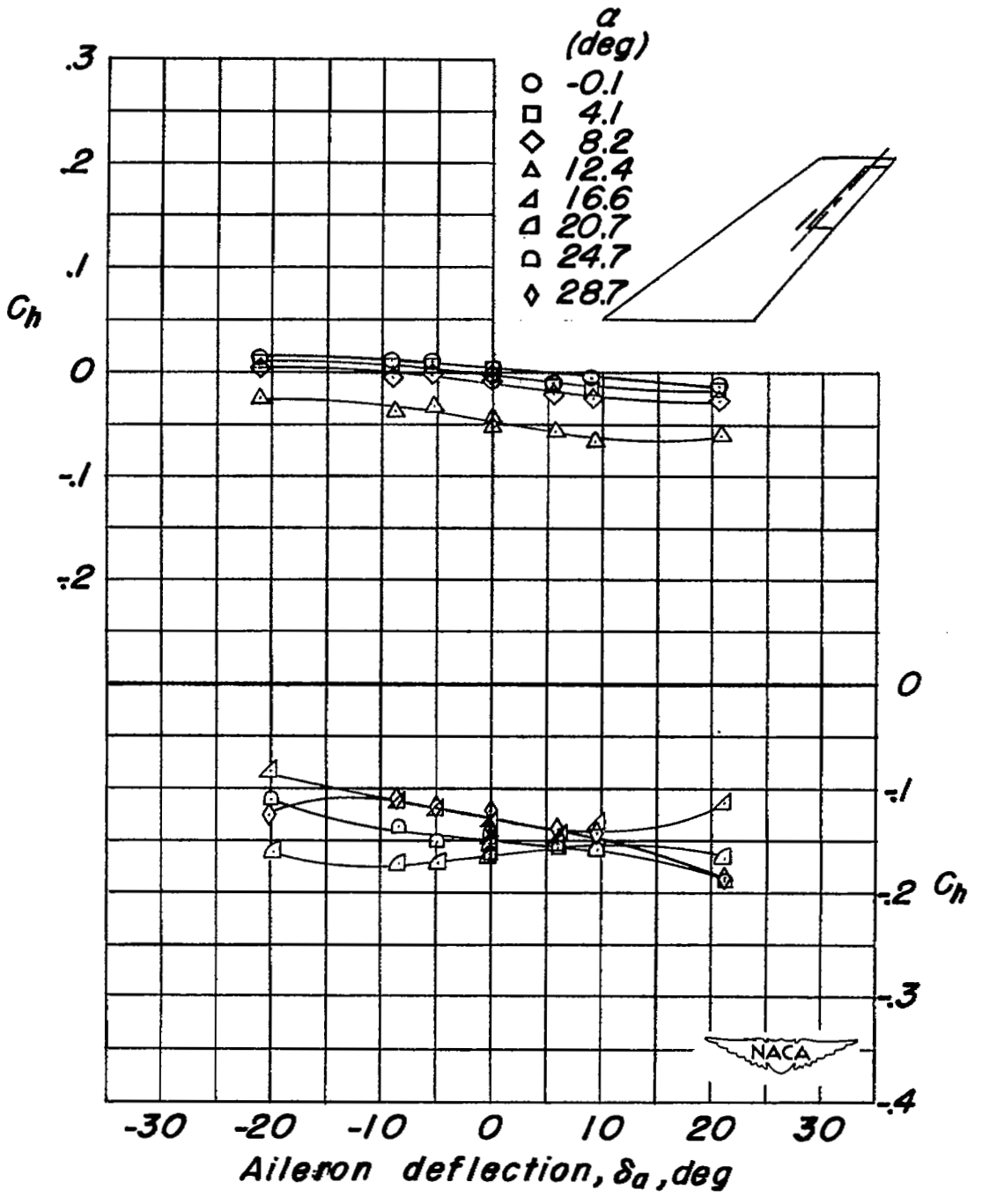

(c) Concluded.

Figure 9.- Continued.

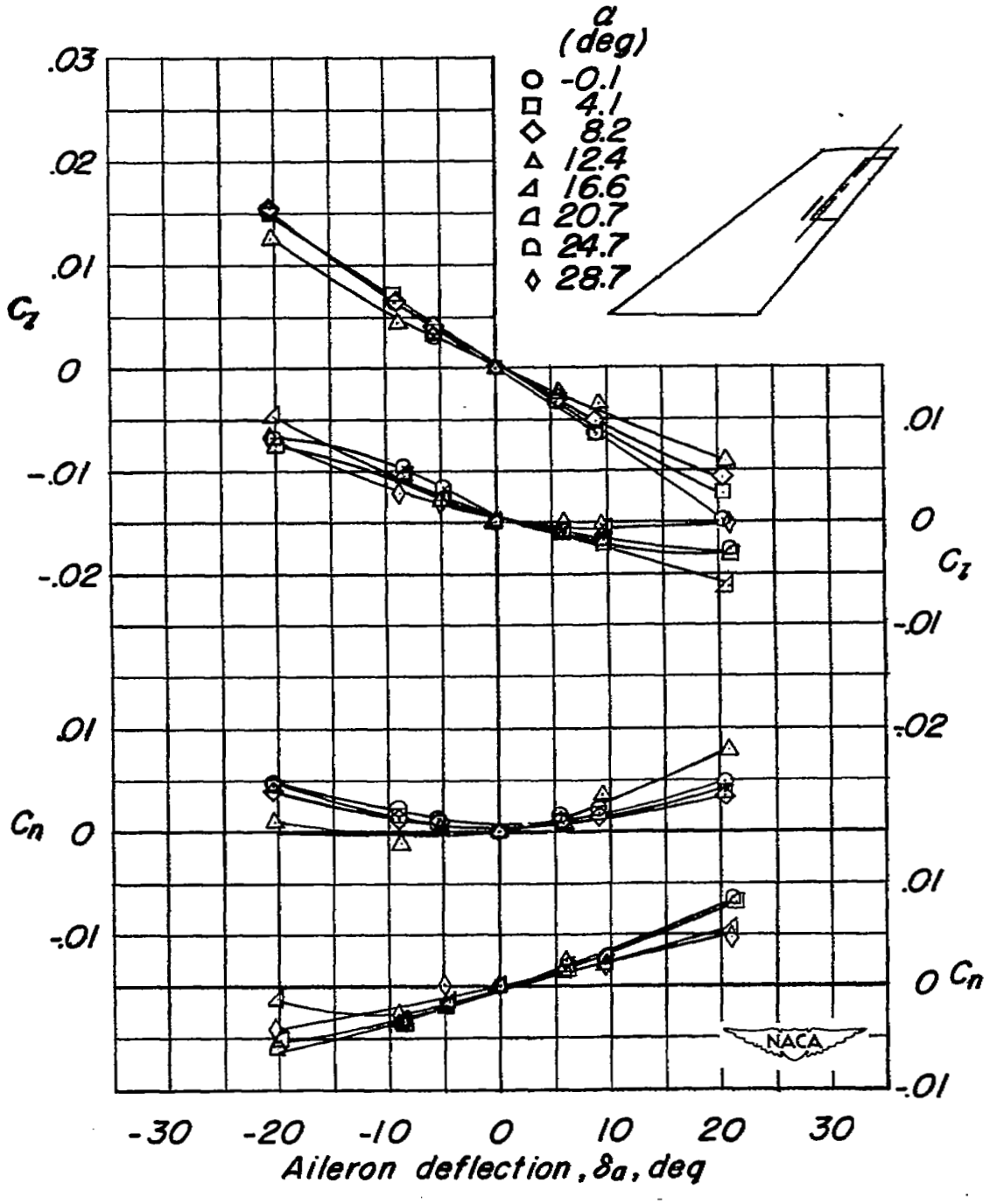

(d) Three-eights-aileron-span spoiler projected 0.02c per 5° δ_a.

Figure 9.- Continued.

[redacted]

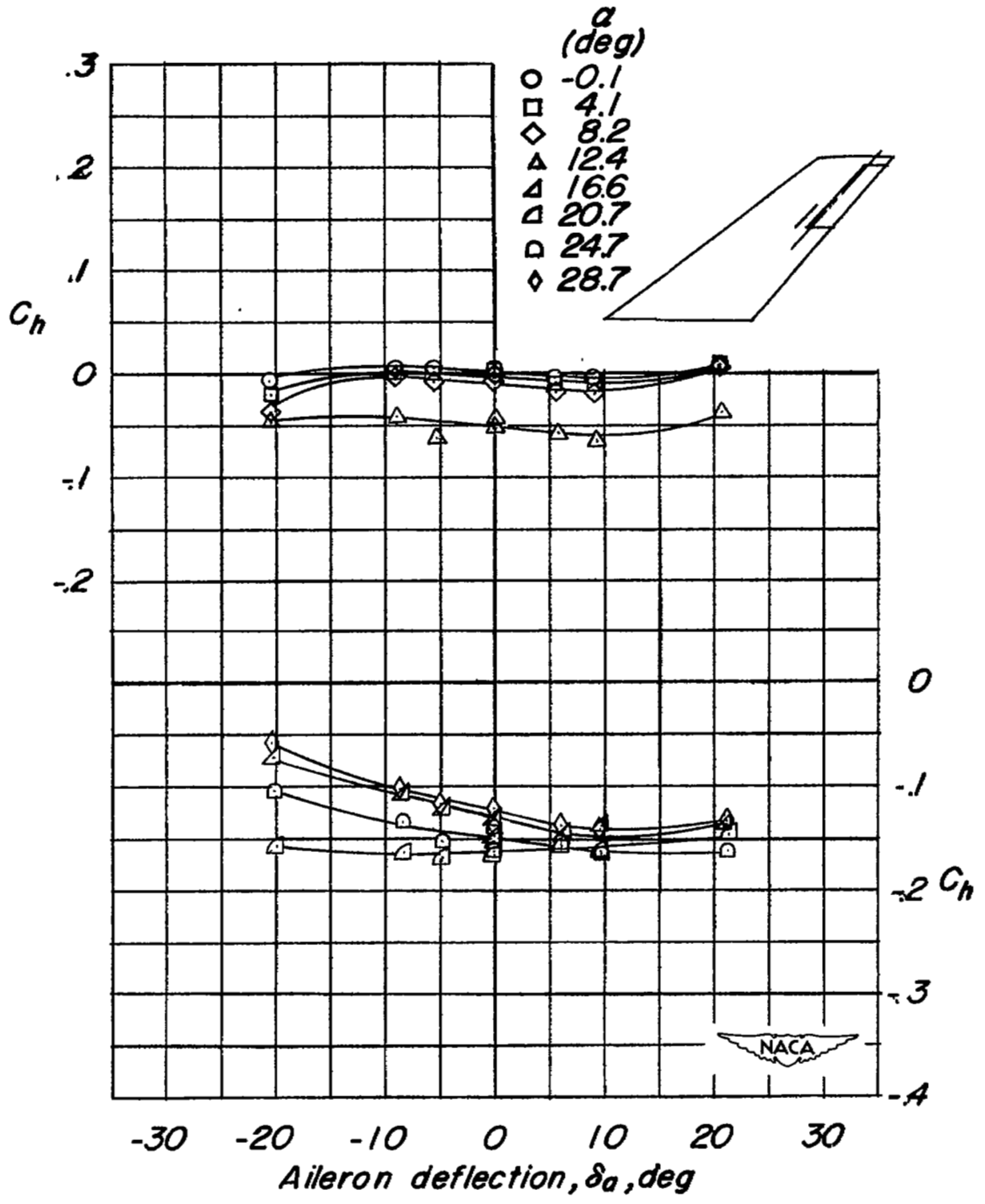

(d) Concluded.

Figure 9.- Continued.

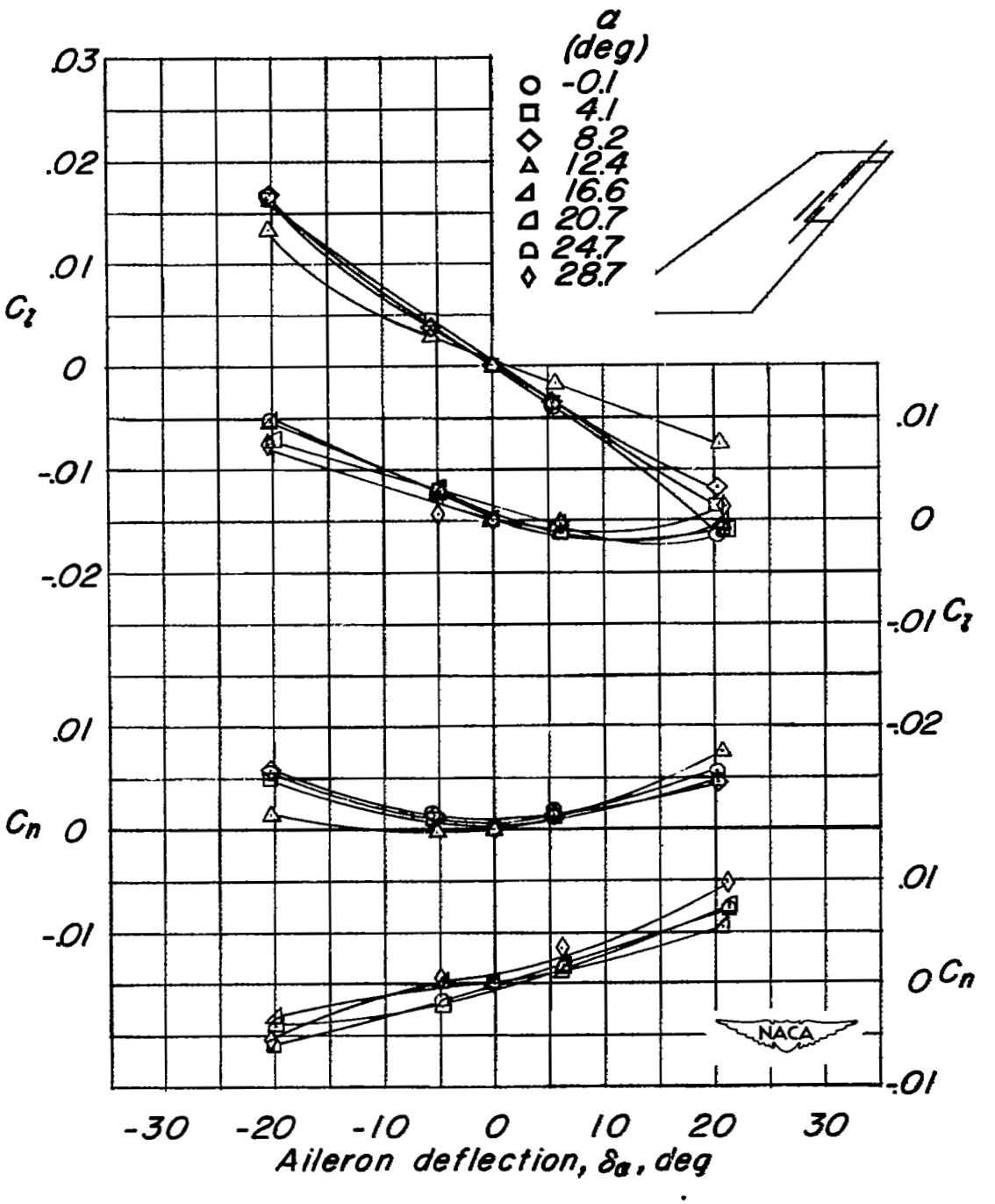

(e) One-half-aileron-span spoiler projected 0.02c per 5° δ_a.

Figure 9.- Continued.

[redacted]

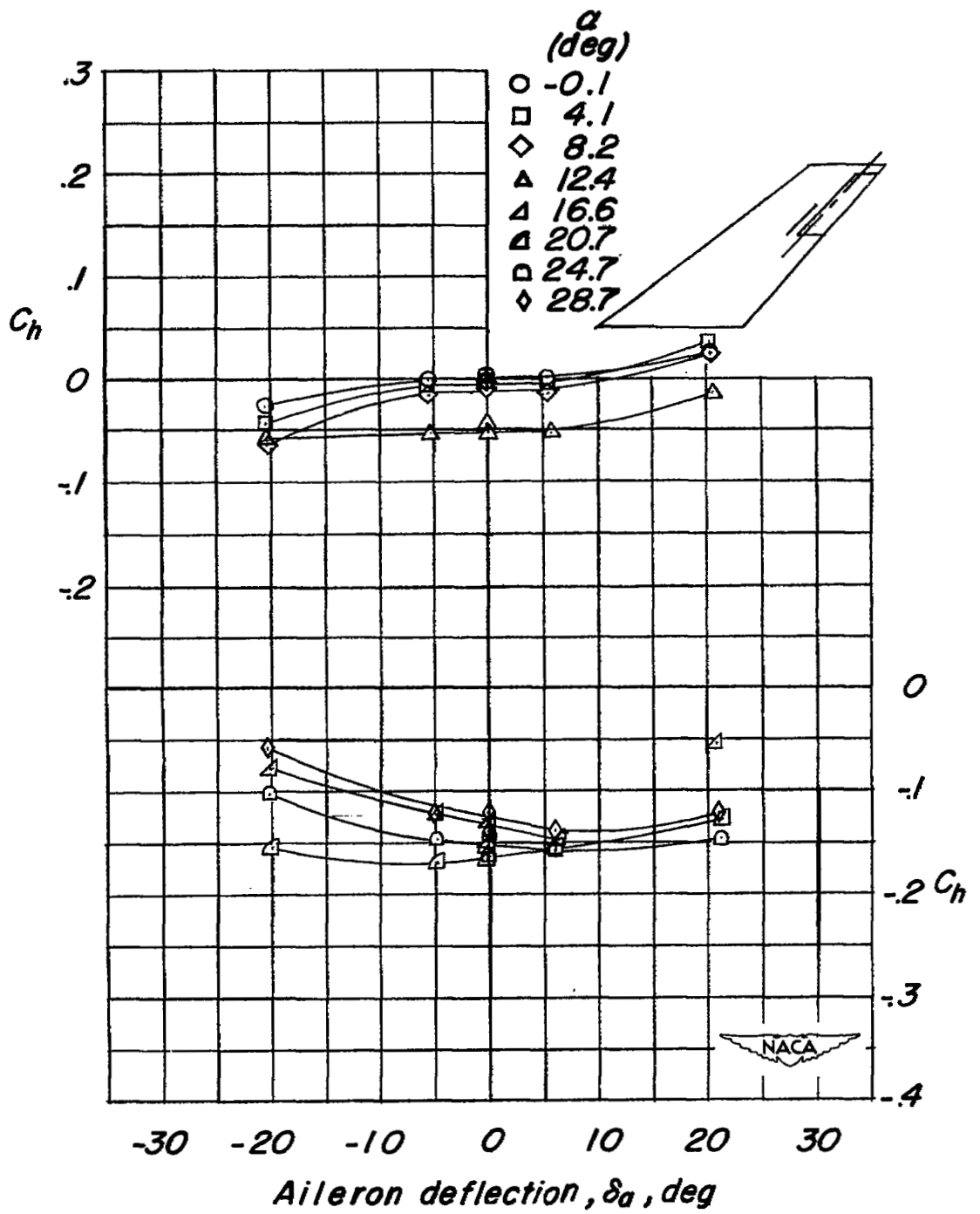

(e) Concluded.

Figure 9.- Concluded.

[redacted]

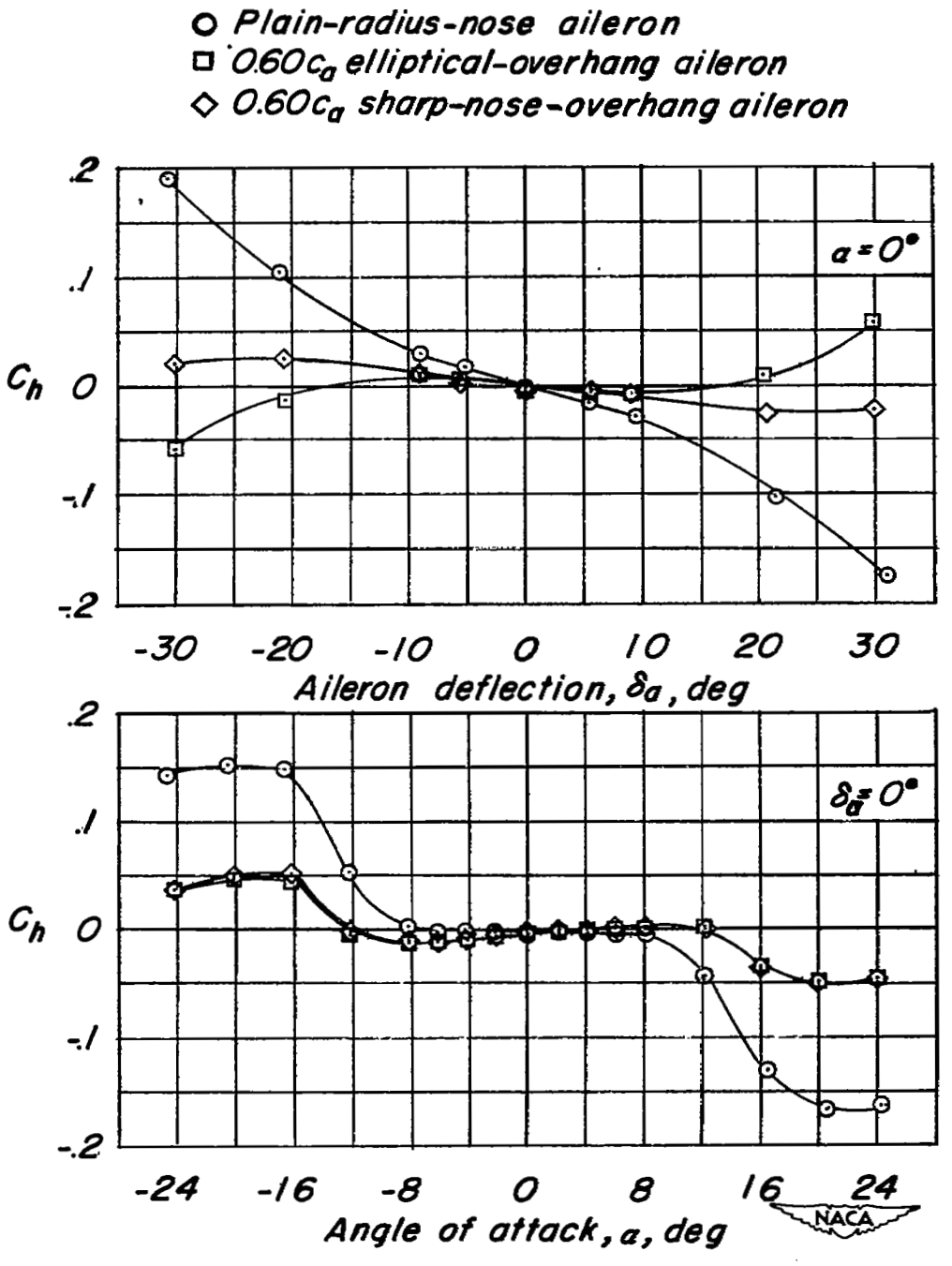

(a) Overhang balances.

Figure 10.- Variation of the lateral-control and hinge-moment characteristics for the plain-radius-nose aileron equipped with various aerodynamic balances.

[redacted]

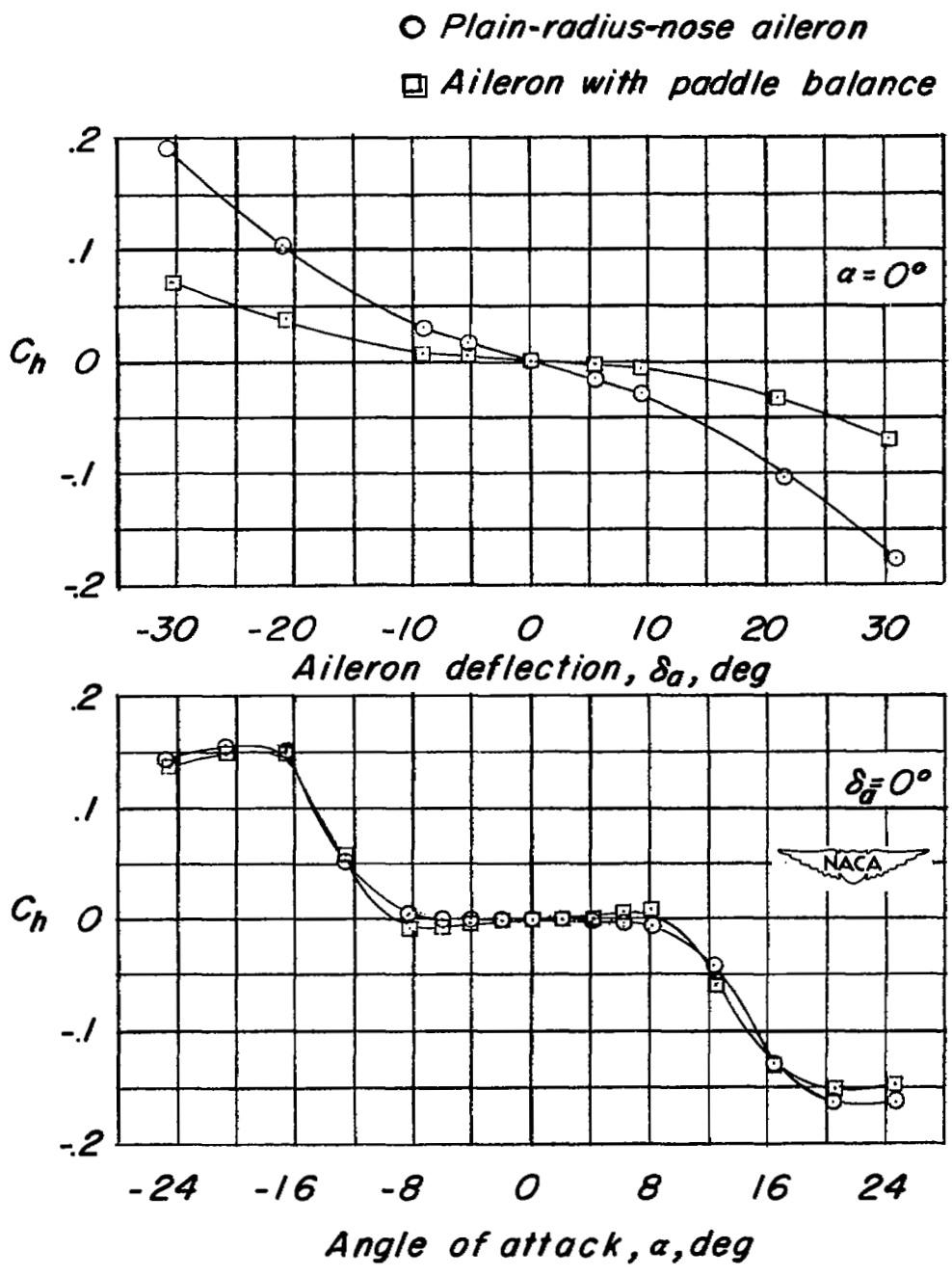

(b) Paddle balances.

Figure 10.- Continued.

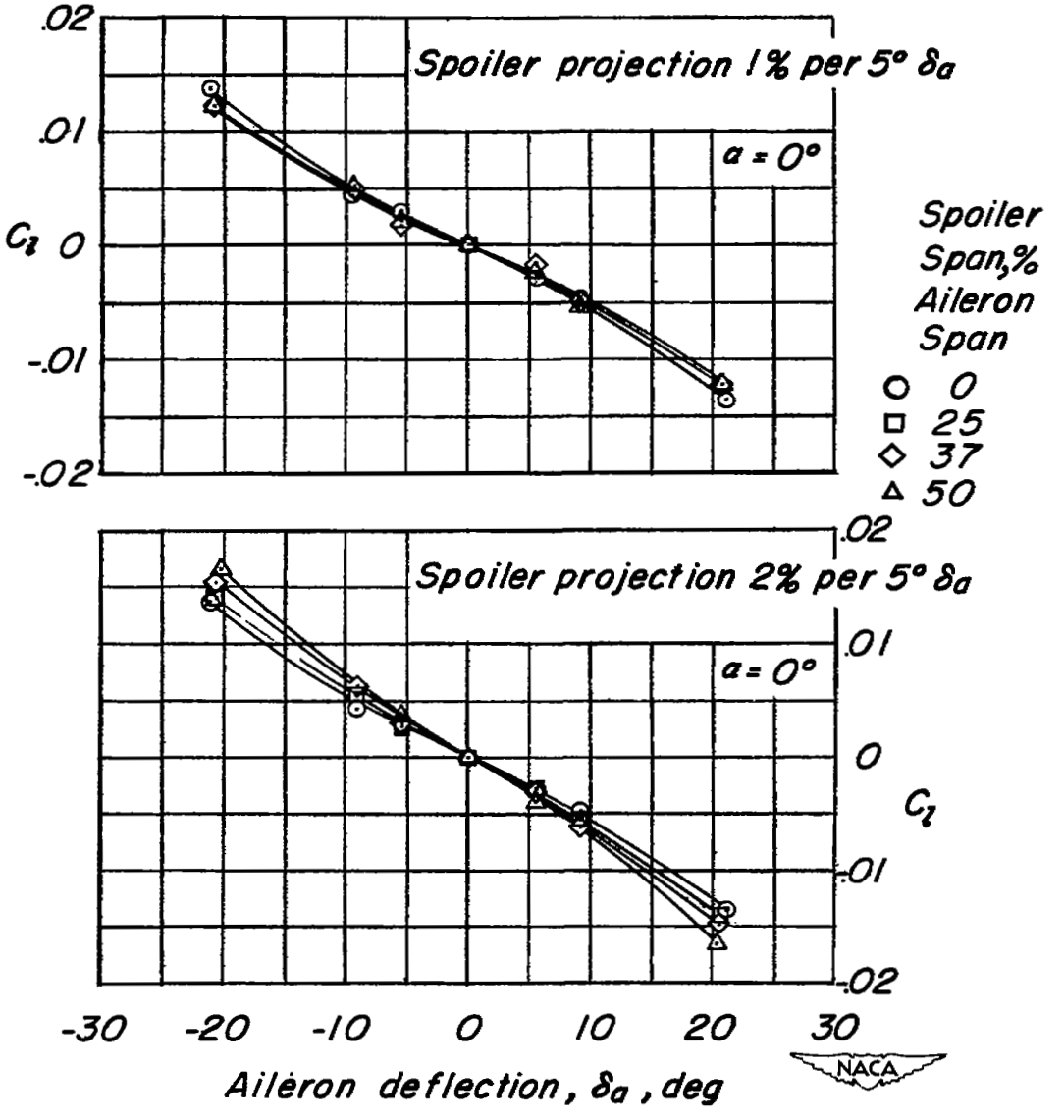

(c) Spoiler balances.

Figure 10.- Continued.

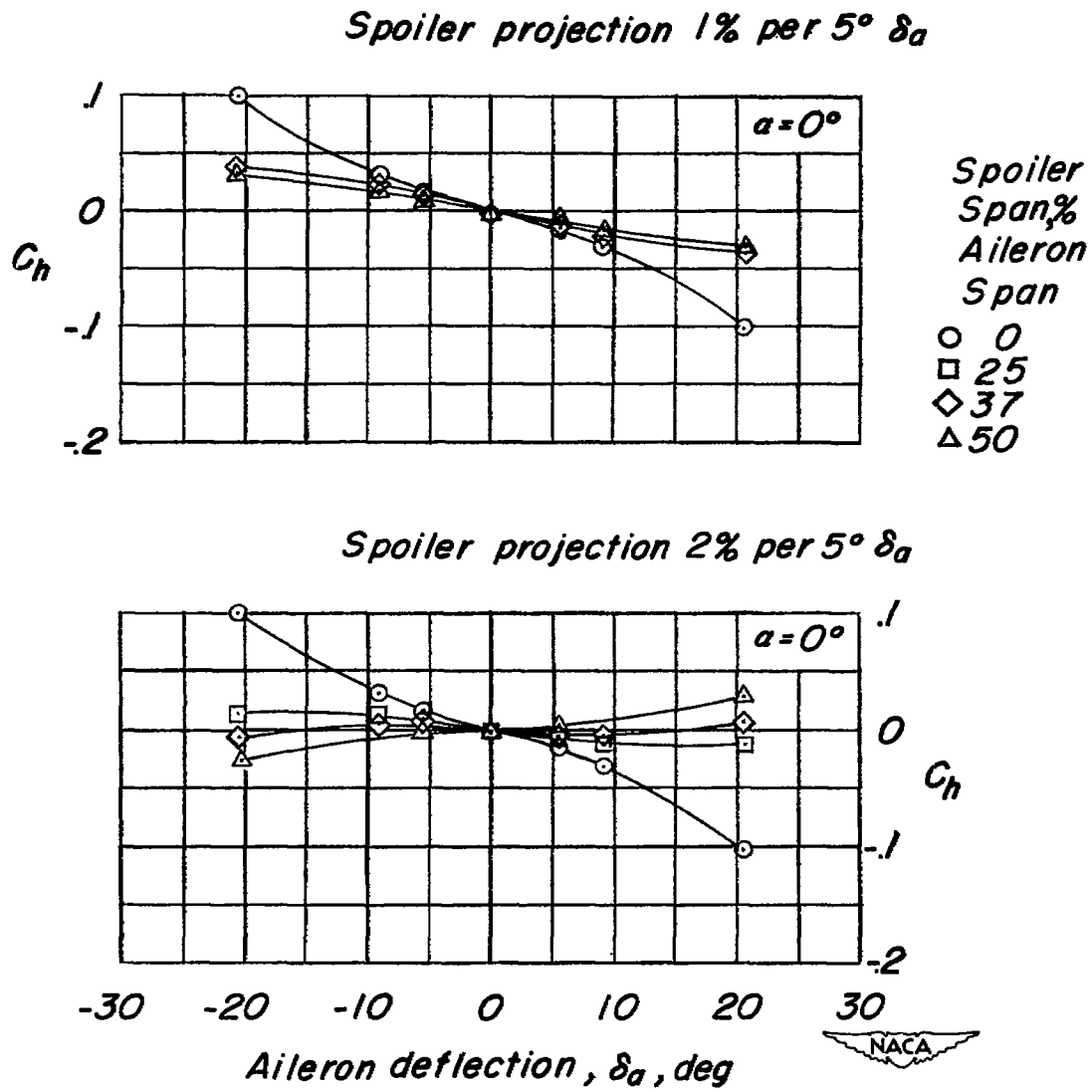

(c) Concluded.

Figure 10.- Concluded.

NACA-Langley - 9-15-52 - 350

[redacted]